

## 2. MESOZOIC CALCAREOUS NANNOFOSSIL BIOSTRATIGRAPHY FROM SITES 897, 899, AND 901, IBERIA ABYSSAL PLAIN: NEW BIOSTRATIGRAPHIC EVIDENCE<sup>1</sup>

Eric de Kaenel<sup>2</sup> and James A. Bergen<sup>3</sup>

### ABSTRACT

Mesozoic calcareous nannofossil assemblages recovered during Ocean Drilling Program Leg 149 from the Iberia Abyssal Plain off the coast of Portugal were examined to determine the age of the rifting processes that affected the western Iberia Margin.

Dark carbonaceous claystones (black shales) recovered from Site 901 contain highly diverse and abundant Tithonian calcareous nannofossil assemblages. Careful examination and documentation of this material has extended the ranges of numerous Jurassic and Cretaceous species and detailed a significant Late Jurassic assemblage turnover observed in the calcareous nannofossil record.

The Lower Cretaceous sequence consists of intervals of serpentinized peridotite intercalated between various breccias and dark claystones. With the exception of a few samples, calcareous nannofossils are few and moderately preserved. The age of nannofossils within these varied sedimentary lithologies ranges from the late Barremian to the late Aptian.

Eight new species are described: *Ansulaspheera covingtonii*, *Clepsilithus meniscus*, *Conusphaera sinespina*, *Crepidolithus parvulus*, *Diazomatholithus galicianus*, *Percivalia arata*, *Rotelapillus pleoseptatus*, and *Tranolithus incus*. Also proposed are five new combinations.

### INTRODUCTION

During Ocean Drilling Program (ODP) Leg 149, five sites were drilled in the Iberia Abyssal Plain, which is located on the eastern North Atlantic, off the coast of Portugal (Fig. 1). Mesozoic sediments were recovered at Sites 897, 899, and 901. The main objective of this cruise was to sample the upper continental and oceanic crusts to determine their origin and history. At Site 901, a high basement block within the ocean/continent transition zone was drilled, and, although recovery was very poor, it yielded one of the most interesting sections to date of lower Tithonian sediments in the North Atlantic. Previous Tithonian sections were recovered by Deep Sea Drilling Project (DSDP) Legs 11, 44, and 76 located in the western North Atlantic, in the Blake-Bahamas Basin off the coast of Florida (Wilcoxon, 1972; Thierstein, 1975; Roth, 1978, 1983; Wind, 1978; Bralower et al., 1989, Bergen, 1994).

Sites 897 and 899 were drilled over basement ridges within the ocean/continent transition zone, and discontinuous sections of upper Barremian to upper Aptian sediments were recovered. Previous studies of Lower Cretaceous nannofossils from the North Atlantic Basin are summarized in Applegate and Bergen (1988) and in Bralower et al. (1989).

The main purpose of this study is to describe the abundance, preservation, and biostratigraphic distribution of Mesozoic calcareous nannofossils recovered during ODP Leg 149. The end of the Jurassic period is marked by a major species radiation and assemblage turnover. Many known Cretaceous species may have originated during the early Tithonian, as documented at Hole 901 A. For this hole, a detailed range chart of the distribution of 110 nannofossil species in this critical interval is presented. Paleoenvironmental influences are indicated based on the observation of certain assemblages with predominantly Boreal nannofossil taxa and the absence of certain Tethyan

taxa. To eliminate taxonomic uncertainties and confirm identifications, a transfer technique was used to illustrate the same specimen with both light and scanning electron microscopes.

### METHODS

In order to obtain good-quality slides, all samples used in this study were prepared using a settling technique. Settling techniques eliminated particles with a size range of <2  $\mu\text{m}$  and >30  $\mu\text{m}$ . In this study, a special settling technique has been developed to prepare slides for the light microscope (LM).

A constant volume of 25 mm<sup>3</sup> of sediment was put into a graduated 15 mL test tube, which was filled with distilled water to 8 mL. The sample was shaken several times within an hour and then held still for 30 s to let the larger particles sink to the bottom. A capillary tube was used to remove the bottom solution down to 3 mL, and water was added to 15 mL. Next, the sample was shaken several times for 5 min and then held still for 90 s. A graduated capillary tube was used to place 8 mL of solution from the top of the tube on a cover slide. Up to 30 samples could be processed at regular intervals during an hour. The same settling technique was used to prepare a gridded circular cover slide for transferring and observing the same specimen in both LM and SEM. Eight drops on a gridded cover slide usually provided a good concentration of nannofossils for both LM and SEM. Twenty-two transferred specimens are illustrated on the 11 plates. The specimen transfer technique used herein was developed by Dr. Frank H. Wind at the Florida State University.

This settling technique, using a constant volume of sediment and solution, has two important advantages. First, it is a relatively quick method, and, second, it causes the coccoliths to disperse on the slides uniformly. Also, occurrences of markers or rare species are found more quickly on a slide prepared by settling rather than on an ordinary smear slide. In this study, this has been very helpful in finding certain rare taxa.

Abundances of individual species in each sample were estimated by using a Zeiss Photomicroscope III under  $\times 1250$  magnification. Seven levels of abundance were recorded used according to the following definitions:

<sup>1</sup>Whitmarsh, R.B., Sawyer, D.S., Klaus, A., and Masson, D.G. (Eds.), 1996. *Proc. ODP, Sci. Results*, 149: College Station, TX (Ocean Drilling Program).

<sup>2</sup>Department of Geology, Florida State University, Tallahassee, Florida 32306-3026, U.S.A. dekaenel@geomag.gly.fsu.edu

<sup>3</sup>Amoco Production Company, 501 West Lake Boulevard, P.O. Box 3092, Houston, Texas 77253, U.S.A.

P (present) = 1 specimen per 201-500 fields of view;  
 R (rare) = 1 specimen per 51-200 fields of view  
 F (few) = 1 specimen per 11-50 fields of view  
 C (common) = 1 specimen per 2-10 fields of view;  
 A (abundant) = 1-10 specimens per field of view;  
 V (very abundant) = 10-100 specimens per field of view;  
 O (ooze) = more than 100 specimens per field of view.

The same definitions are used for estimates of total abundance in each sample, with an added definition: B (barren of nannofossils).

The following estimates are based on the comments of Roth and Thierstein (1972). The qualitative evaluation of the preservation of calcareous nannofossils was denoted as follows:

P (poor) = severe dissolution, fragmentation and/or overgrowth have occurred; most primary features have been destroyed and many specimens cannot be identified at the species level;  
 M (moderate) = Dissolution and/or overgrowth are evident; a significant proportion (up to 25%) of the specimens cannot be identified to species level with absolute certainty;  
 X (mixed) = Dissolution and/or overgrowth are evident among certain taxa, but nearly all specimens (up to 95%) can be identified with certainty;  
 G (good) = Little dissolution and/or overgrowth is seen; diagnostic characteristics are preserved and all specimens can be identified;  
 E (excellent) = No dissolution is observed; all specimens can be identified.

## SITE SUMMARY AND BIOSTRATIGRAPHY

Nannofossil distributions in the four Mesozoic sections drilled during Leg 149 on the Iberia Abyssal Plain (Table 1) are given in Tables 2-5 and their locations in Figure 1.

### Tithonian: Hole 901A

Nearly all the "standard" Late Jurassic marker species are present in the thin Jurassic section drilled at Site 901. A detailed description of the nannofossil assemblage is given in Table 2. The most distinct calcareous nannofossil events in this section are indicated in the second column from the left of the nannofossil distribution chart (Table 2) and of the summary range chart (Fig. 2). Relative stratigraphic ranges of key calcareous nannofossil species events are shown in Figure 2.

Hole 901A was cored intermittently and seven cores recovered only 7.67 m of sediments. The Tithonian interval is found from the top of Core 149-901A-3R to Core 149-901A-7R. About 20 m of sediment was washed within this interval, and recovery in the other cores investigated averaged about 13% (see Fig. 2). However, this site does provide important biostratigraphic data. The lithology of this interval consists of 90% olive-black claystone with some intercalations of thin silt laminae and black plant debris and 10% parallel-laminated calcareous sandstones.

Lower and upper intervals are defined by the calcareous nannofossil assemblages. The lower interval from Cores 149-901A-5R through 7R contains rare to highly diverse, poorly to moderately well-preserved assemblages. Sample 149-901A-5R-1, 31 cm, which contains a moderately well-preserved assemblage, yielded about 95 nannofossil species. This lower interval belongs to the lower Tithonian. The upper interval (Core 149-901A-3R) contains essentially the same diversity, poorly to moderately well-preserved nannofossil assemblages. A late Tithonian age is indicated by the FOs of several markers and the presence of species restricted to the Jurassic (see below, biozonations). Six forms observed in Core 149-901A-3R have never been reported in Jurassic sediments, including *Duplexipodor-*

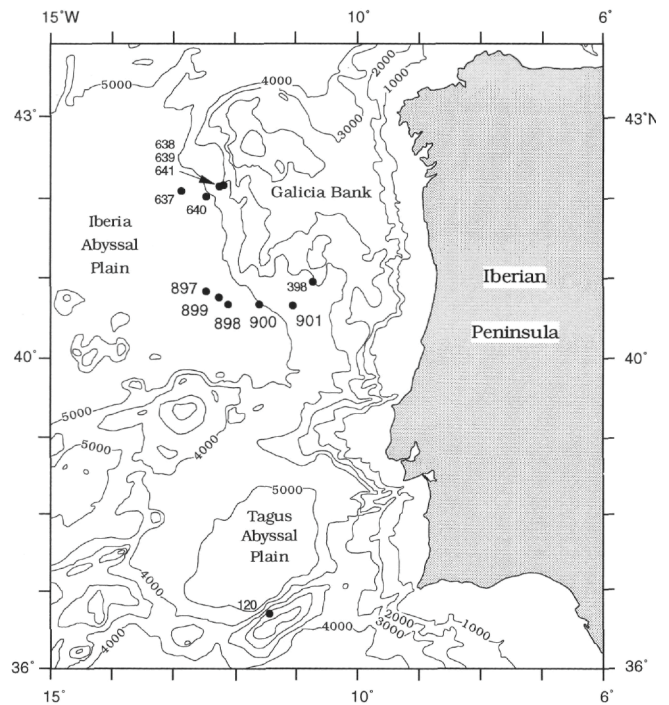


Figure 1. Site location map of the Iberia Abyssal Plain showing ODP Leg 149 Sites 897 to 901. Site 398 (DSDP Leg 47) and Sites 637 to 641 (ODP Leg 103) are indicated for reference.

*habdus plethotretus*, *Ethmorhabdus hauterivianus*, *Grantarhabdus bukryi*, *Perissocyclus noeliae*, *Perissocyclus tayloriae*, and *Perissocyclus fletcheri* (Fig. 2). Also reported for the first time in Jurassic sediments is the genus *Percivalia*. The FOs of *Percivalia arata* (new species) and *Pickelhaube furtiva* are two distinct events near the top of the lower interval.

Because the period of time represented in these two Tithonian intervals is relatively short, shown in Figure 2 and Table 2 are calcareous nannofossil events, instead of zonal codes. These nannofossil events are defined by species that have been selected for their typical, and easily identifiable, morphologies, and they are used to subdivide the Tithonian interval recovered in Hole 901 A.

### Biozonations

Both the Jurassic biozonation for northwestern Europe (Bown et al., 1988; NJ Zones) and the Tithonian biozonation based on southern Europe and the western North Atlantic (Bralower et al., 1989; NJ and NJK Zones) are broadly applicable to Hole 901 A, although certain index species are either absent or have extended stratigraphic ranges in this section. The NJ Zones of Bralower et al. (1989) are not comparable to the NJ Zones of Bown et al. (1988). Redeposition seems a plausible explanation for the observed stratigraphic range extensions, but this seems valid only for the rare and isolated occurrences of older Late Jurassic taxa (e.g., *Axopodorhabdus rahla*). In contrast, the near absence of certain taxa in this section (e.g., *Nannoconus*) cautions toward possible paleogeographic controls on the stratigraphic ranges of remaining problematic species (e.g., *Stephanolithion bigotii*). Secondary biostratigraphic events illustrated by Bralower et al. (1989) indicate an early to late Tithonian age for the sediments recovered at Site 901 (Zone NJK).

An age no older than Tithonian is indicated by the presence of *Zeugrhabdus embergeri*, *Conusphaera mexicana mexicana*, *Conusphaera mexicana minor*, and "*Polycostella beckmanii*" at the base of the section (Sample 149-901A-7R-1, 32cm). Observed spec-

**Table 1. Location of ODP Leg 149 sites where Mesozoic sediments were recovered.**

Hole	Latitude (°N)	Longitude (°W)	Water depth (m)
897C	40°50.32'	12°28.44'	5320
897D	40°50.31'	12°28.51'	5315
899B	40°46.34'	12°16.06'	5291
901A	40°40.47'	11°03.58'	4718

imens of *Polycostella beckmanii* are similar to detached spines of *Conusphaera mexicana minor* (see *C. mexicana minor* in Appendix A). Both *Microstaurus chiastus* and *Markalius ellipticus* are present near the base of the section (Sample 149-901A-7R-1, 14 cm). The first occurrence (FO) of *M. chiastus* defines the base of Zone NJK of Bralower et al. (1989) and the FO of *M. ellipticus* is indicated as a secondary event within the upper part of Subzone NJK-A. The definitive presence of an upper Tithonian section is indicated by the FOs of four species at the very top of Core 149-901A-3R: *Cruciellipsis cuvillieri*, *Manivitella pemmatoidea*, *Rhagodiscus asper*, and *Rotelapillus laffitei* (Fig. 2). The latter event defines the base of Subzone NJK-C of Bralower et al. (1989). Delineation of Subzones NJK-A and NJK-B of Bralower et al. (1989) in the underlying section was not possible because of the absence of *Umbria granulosa granulosa* in Hole 901 A, although the ancestral subspecies *Umbria granulosa minor* was observed in three isolated samples (see Table 2). Also present in the section is *Stephanolithion atmetros*. The FO of this species defines the base of Zone NJ17 of Bown et al. (1988) and has been correlated to the upper Kimmeridgian (sensu anglico) Pallasioides ammonite Zone in northwest Europe.

Three species ranging throughout the section in Hole 901A (Fig. 2) indicate an age no younger than Tithonian: *Ellipsagelosphaera reinhardtii*, *Hexapodorhabdus cuvillieri*, and *Stephanolithion bigotii*. The distribution of *Faviconus multicolumnatus* is more sporadic, but a single specimen was observed in the uppermost Sample 149-901A-3R-1, 1 cm. Bralower et al. (1989) showed the extinction of *Faviconus multicolumnatus* within their Tithonian Subzone NJK-B and placed its last occurrence (LO) in DSDP Hole 534A in Core 92-6, 147 cm. Bergen (1994) reported the LO for this species in Core 92-1, 79-80 cm in DSDP Hole 534A (top Subzone NJK-B), but correlated this horizon to the basal Cretaceous *jacobi* ammonite Zone in southeastern France. The extinctions of *Ellipsagelosphaera reinhardtii* and *Hexapodorhabdus cuvillieri* seem problematic, but these are less reliable bioevents. The LO of *E. reinhardtii* is a new bioevent. It was observed farther downsection in Hole 534A (Core 94-1, 93-94 cm; Subzone NJK-A of Bralower et al., 1989), but not above the lower Tithonian *fallauxi* Zone in two sections (Route de Grads, Carrière des Anges) near Le Pouzin in southeastern France (J.A. Bergen, pers. obs., 1991). *H. cuvillieri* has limited biostratigraphic utility largely because of the delicate construction of its central area. However, its LO in Hole 534A was observed in Core 95-2, 20-21 cm (J.A. Bergen, pers. obs., 1991; Subzone NJK-A of Bralower et al., 1989). Wind (1978) also illustrated a LO for this species in DSDP Hole 391C in Core 49-2, 72 cm, which Bralower et al. (1989) later placed within their NJ20 Zone. The most problematic bioevent in Hole 391C is the extinction of *Stephanolithion bigotii*. Bralower et al. (1989) indicated the extinction of *S. bigotii* prior to the appearance of *Conusphaera mexicana mexicana* (base of Subzone NJ20B) and showed these events in proximity to the Kimmeridgian/Tithonian boundary. In Hole 901 A, both species range throughout the short interval examined (Table 2). Additionally, numerous specimens of *S. bigotii* were observed in the two uppermost samples examined (Table 2), both of which contain the aforementioned late Tithonian nannofossil index species (see previous paragraph). Redeposition seems an unlikely explanation, as *Stephanolithion bigotii* was found in good abundance throughout the section. One possible explanation is offered by more

tentative correlations to northwest Europe, for which Bown et al. (1988) illustrated an overlap in the stratigraphic ranges of *S. bigotii* and *S. atmetros* (FO defines the base of Zone NJ17) only within the upper Kimmeridgian (sensu anglico) *pallasioides* ammonite Zone. Both nannofossil species are present in Hole 901A (Table 2). The most recent version of the Jurassic sea level chart (Graciansky et al., unpubl. data) shows the Boreal *pallasioides* ammonite Zone correlative to the Tethyan *microcanthum* Zone ("*simplisphinctes* Subzone") of late Tithonian age. Therefore, the extinction of *Stephanolithion bigotii* could be younger in Boreal outcrop sections and at Site 901, suggesting that the species is sensitive to paleoenvironmental conditions and less tolerant of carbonate-rich intervals. Dark, laminated silty claystones recovered from Hole 901A contain Tithonian benthic foraminifer assemblages that indicate a neritic depositional environment with increased organic flux (Collins et al., this volume).

### Paleoecology

At Hole 901 A, microliths and non-imbricated placoliths are dominant. The nannofossil assemblages in the lower Tithonian interval contain several *Stradnerlithus* species described from northern Europe sections and rarely reported from Tethyan sections. The Hole 901A nannofossil assemblages contain common *Conusphaera*, but are conspicuous in the almost complete absence of another Tethyan genus, *Nannoconus*. Bralower et al. (1989) illustrated the presence of *Nannoconus* (*N. compressus*) in two western North Atlantic DSDP Sites (Hole 391C and Hole 534A) together with *Conusphaera mexicana mexicana* and *Polycostella beckmanii* (Subzone NJ20B, which predates *Microstaurus chiastus*, Zone NJK). All three species are present in Hole 901 A. Only very rare, small *Nannoconus* spp. (early forms of *Nannoconus globulus*) have been observed in the upper part of Section 149-901A-3R-1. The absence of *Hexalithus* and *Polycostella senaria* is less conspicuous, but, together with *Nannoconus*, could indicate some paleogeographic segregation from the Tethys (e.g., southeastern France, Spain, and northern Italy). However, these taxa (*N. compressus*, *P. senaria*, *Hexalithus* spp.) also have short stratigraphic ranges and their absence could also indicate a possible hiatus in the section.

### Redeposition

Isolated occurrences of *Axopodorhabdus rahla* (Core 149-901A-5R-1, 31 cm) and *Tubirhabdus patulus* (Samples 149-901A-5R-1, 31 cm, 149-901A-3R-1, 2 cm) may represent redeposited Oxfordian or pre-Oxfordian specimens. Specimens of *Lotharingius sigillatus* in five samples from Cores 5R-7R may be in situ, although this genus is thought to have an Oxfordian extinction (Bown et al., 1988). Bralower et al. (1989) showed isolated occurrences of *Watznaueria crucicentralis* (= *Lotharingius*) in the Tithonian section of Hole 534A. Similarly, Bown et al. (1988) extended the stratigraphic range of *Tubirhabdus patulus* into the upper Kimmeridgian (sensu anglico) in northern Europe. The taxa *Calcivascularis* sp. 1 and *Vagalapilla* sp. 3 were recently observed from the Oxfordian/Kimmeridgian boundary interval in Portugal (Bergen, in press) and are restricted to the Kimmeridgian section in southeastern France and DSDP Hole 534A (J.A. Bergen, pers. obs., 1991). Isolated specimens of these taxa present in three samples (see Table 2) may also be redeposited.

### Upper Barremian to Upper Aptian: Holes 897C, 897D, and 899B

#### Biozonation

Upper Barremian to lower upper Aptian nannofossils were recovered at Holes 897C and 897D, whereas lower Aptian assemblages were recovered from Hole 899B. Zonal assignments are based prima-

Table 2. Stratigraphic distribution of calcareous nannofossil taxa from Hole 901A.

Age	Calcareous Nannofossil Appearance Events	Core, section, interval (cm)	Depth (mbsf)	Abundance	Preservation	<i>Ariifactus harrisonii</i>	<i>Anulusphaera couvignoni</i>	<i>Axopodorhabdus cylindricus</i>	<i>Axopodorhabdus depravatus</i>	<i>Axopodorhabdus ralla</i>	<i>Axopodorhabdus</i> sp., small	<i>Biscutum rotatorium</i>	<i>Braurudosphaera regularis</i>	<i>Calciavicularis</i> sp. 1	<i>Calyculus</i> sp., large	<i>Chiasfozgyus leptostaurus</i>	<i>Clepsilithus mentiscus</i>	<i>Conusphaera mexicana minor</i>	<i>Conusphaera mexicana minor</i> (cir.)	<i>Conusphaera mexicana minor</i> (ell.)	<i>Conusphaera mexicana mexicana</i>	<i>Conusphaera sinespina</i>	<i>Crepidolithus parvulus</i>	<i>Cretarhabdus conicus</i>	<i>Crucellipsis cuvillieri</i>	<i>Cyclagelosphaera deflandrei</i> var. A	<i>Cyclagelosphaera deflandrei</i> var. B	<i>Cyclagelosphaera lacuna</i>	<i>Cyclagelosphaera margeritii</i>	<i>Cyclagelosphaera uietnamitii</i>	<i>Diadorhombus scutulatus</i>	<i>Diazomatolithus galicianus</i>	<i>Diazomatolithus lehrmanii</i>	<i>Discorhabdus patulus</i>			
Tithonian	<i>R. laffitei</i>	3R-1. 1	191.31	A X	X	.	F	R	.	.	F	.	.	.	.	.	F	F	R	F	P	R	R	R	R	P	R	.	F	P	.	F	R	R			
	<i>M. pennatoidea</i>	3R-1. 2	191.32	A X	.	C	F	.	.	.	R	F	.	P	P	.	F	R	F	F	R	F	R	F	P	P	.	R	C	R	.	F	R	R			
		3R-1. 7-8	191.37	C M	.	.	.	.	.	.	.	P	.	.	.	.	.	.	.	.	.	.	.	.	.	.	.	.	F	.	.	.	.	.	.		
		3R-1. 17	191.47	B	.	.	.	.	.	.	.	.	.	.	.	.	.	.	.	.	.	.	.	.	.	.	.	.	.	.	.	.	.	.	.	.	
		3R-1. 33	191.63	A M	.	F	P	.	.	.	F	.	P	.	.	.	F	P	.	.	.	.	.	.	.	.	.	.	F	.	.	R	.	.	.		
		3R-1. 52	191.82	C P	.	F	.	.	.	.	.	.	.	.	.	.	P	.	.	.	.	.	.	.	.	.	P	.	C	.	P	.	.	.	.		
		3R-1. 74-75	192.04	P P	.	.	.	.	.	.	.	.	.	.	.	.	.	.	.	.	.	.	.	.	.	.	.	.	.	.	.	.	.	.	.	.	.
		3R-1. 84	192.14	R P	.	.	.	.	.	.	.	.	.	.	.	.	.	.	.	.	.	.	.	.	.	.	.	.	.	.	.	.	.	.	.	.	.
	4R-1. 6	200.86	B	.	.	.	.	.	.	.	.	.	.	.	.	.	.	.	.	.	.	.	.	.	.	.	.	.	.	.	.	.	.	.	.	.	
	4R-1. 31	201.11	B	.	.	.	.	.	.	.	.	.	.	.	.	.	.	.	.	.	.	.	.	.	.	.	.	.	.	.	.	.	.	.	.	.	
	<i>P. furtiva</i>	5R-1. 31	220.11	A X	R	F	F	.	P	R	F	P	P	R	R	R	F	F	F	F	P	F	R	F	P	.	P	P	R	P	.	P	F	F	F		
	<i>P. arata</i>	5R-1. 49-50	220.29	R P	.	.	.	.	.	.	.	.	.	.	.	.	.	F	F	F	.	F	.	.	.	.	.	.	P	.	.	F	.	F	.	F	
		5R-1. 74	220.34	A X	F	F	F	.	.	.	R	F	.	.	.	.	.	F	F	F	.	F	.	.	.	.	.	.	F	.	.	F	.	F	.	F	
	<i>G. bukryi</i>	5R-1. 108	220.88	C M	.	R	.	.	.	.	R	.	.	.	.	.	.	.	.	.	.	.	.	.	.	.	.	.	F	.	.	.	.	.	P	.	.
		5R-2. 17	221.47	C M	.	R	.	.	.	.	R	.	.	.	.	.	R	P	.	.	.	.	.	.	.	.	.	.	F	.	.	.	.	.	.	.	.
		6R-1. 42	229.82	A M	.	C	.	.	.	.	P	F	.	.	.	.	R	F	R	R	.	R	.	F	.	.	.	.	F	.	P	.	P	.	.	.	.
		6R-1. 119	230.59	C M	.	R	.	.	.	.	.	.	.	.	P	.	.	.	.	.	.	.	.	.	.	.	.	.	R	.	.	.	.	.	.	.	.
	<i>M. ellipticus</i>	7R-1. 10	238.20	B	.	.	.	.	.	.	.	.	.	.	.	.	.	.	.	.	.	.	.	.	.	.	.	.	.	.	.	.	.	.	.	.	.
7R-1. 14		238.24	A X	.	F	R	P	.	.	F	.	.	.	.	.	F	R	F	.	R	.	R	P	.	.	.	R	F	.	R	F	R	R	.	.		
7R-1. 32		238.42	A M	.	F	R	.	.	.	R	.	.	.	.	.	F	F	R	.	R	.	R	R	.	.	.	F	P	.	R	.	R	.	R	.		

Age	Calcareous Nannofossil Appearance Events	Core, section, interval (cm)	Depth (mbsf)	Abundance	Preservation	<i>Sollasites horticus</i>	<i>Stephanolithion atretos</i>	<i>Stephanolithion bigotii</i>	<i>Stradnerithus asymmetricus</i>	<i>Stradnerithus comptus</i>	<i>Stradnerithus sexstratus</i>	<i>Tetrapodorhabdus coptensis</i>	<i>Thoracosphaera</i> sp. 1	<i>Thurmannolithion claratum</i>	<i>Tranolithus incus</i>	<i>Triscutum</i> cf. <i>T. expansum</i>	<i>Procolithus charlotet</i>	<i>Truncatoscapus senarius</i>	<i>Tubirhabdus patulus</i>	<i>Umbria granulosa minor</i>	<i>Vagalapilla parella</i>	<i>Vagalapilla quadratocula</i>	<i>Vagalapilla</i> sp. 1	<i>Vagalapilla</i> sp. 3	<i>Vagalapilla stradneri</i>	<i>Watznaueria barnesae</i>	<i>Watznaueria fossacincta</i>	<i>Watznaueria manniatae</i>	<i>Watznaueria ovata</i>	<i>Watznaueria tubulata</i>	<i>Zeugrhabdotus choffatii</i>	<i>Zeugrhabdotus embergeri</i>	<i>Zeugrhabdotus erectus</i>	<i>Zeugrhabdotus erectus</i> (thick bar)	<i>Zeugrhabdotus fissus</i>	<i>Zeugrhabdotus noeliae</i>			
Tithonian	<i>R. laffitei</i>	3R-1. 1	191.31	A X	X	.	.	F	P	.	.	F	.	.	.	P	P	.	P	.	.	R	.	P	F	F	F	R	R	P	R	F	R	C	R				
	<i>M. pennatoidea</i>	3R-1. 2	191.32	A X	.	F	R	.	.	.	P	R	.	R	P	P	.	.	P	.	.	.	P	R	.	P	C	F	P	R	.	R	R	F	R	C	R		
		3R-1. 7-8	191.37	C M	.	.	.	.	.	.	.	.	.	.	.	.	.	.	.	.	.	.	.	.	.	.	F	C	.	.	.	P	R	.	R	.	.		
		3R-1. 17	191.47	B	.	.	.	.	.	.	.	.	.	.	.	.	.	.	.	.	.	.	.	.	.	.	.	.	.	.	.	.	.	.	.	.	.	.	
		3R-1. 33	191.63	A M	.	.	P	.	.	.	.	.	.	.	.	.	.	R	.	.	.	.	.	.	.	.	R	.	.	.	R	R	F	.	.	.	.		
		3R-1. 52	191.82	C P	.	.	.	.	.	.	.	.	.	.	.	.	.	.	.	.	.	.	.	.	.	.	F	R	P	.	.	P	R	.	F	.	.	.	
		3R-1. 74-75	192.04	P P	.	.	.	.	.	.	.	.	.	.	.	.	.	.	.	.	.	.	.	.	.	.	P	.	.	.	.	.	.	.	.	.	.	.	
		3R-1. 84	192.14	R P	.	.	.	.	.	.	.	.	.	.	.	.	.	.	.	.	.	.	.	.	.	.	R	.	.	.	.	.	.	.	.	.	.	.	
	4R-1. 6	200.86	B	.	.	.	.	.	.	.	.	.	.	.	.	.	.	.	.	.	.	.	.	.	.	.	.	.	.	.	.	.	.	.	.	.	.	.	
	4R-1. 31	201.11	B	.	.	.	.	.	.	.	.	.	.	.	.	.	.	.	.	.	.	.	.	.	.	.	.	.	.	.	.	.	.	.	.	.	.	.	
	<i>P. furtiva</i>	5R-1. 31	220.11	A X	R	R	F	F	F	F	R	P	F	P	P	P	P	P	P	P	P	R	F	F	R	C	C	R	R	P	.	R	C	F	C	R			
	<i>P. arata</i>	5R-1. 49-50	220.29	R P	.	.	.	.	.	.	.	.	.	.	.	.	.	.	.	.	.	.	.	.	.	.	P	.	F	F	P	P	.	F	R	R	R	C	.
		5R-1. 74	220.34	A X	.	.	R	F	.	.	F	P	.	P	.	.	R	.	.	.	.	.	F	F	P	F	F	C	P	P	.	F	R	R	R	C	.		
	<i>G. bukryi</i>	5R-1. 108	220.88	C M	.	.	.	.	.	.	.	.	.	.	.	.	.	.	.	.	.	.	.	.	.	.	F	F	.	P	.	R	P	P	.	F	.	.	.
		5R-2. 17	221.47	C M	.	.	P	.	.	.	.	.	.	.	.	.	.	.	.	.	.	.	.	.	.	.	R	F	.	.	F	.	.	F	.	.	.	.	
		6R-1. 42	229.82	A M	.	.	R	P	.	.	P	.	.	.	.	.	.	R	.	.	.	.	.	.	.	R	P	P	F	.	R	P	R	.	C	.	.	.	
		6R-1. 119	230.59	C M	.	.	.	.	.	.	.	.	.	.	.	.	.	.	.	.	.	.	.	.	.	.	F	F	.	.	.	.	.	.	.	.	.	.	.
	<i>M. ellipticus</i>	6R-1. 131	230.71	A X	P	P	F	P	.	.	P	.	.	.	.	.	P	.	.	.	.	.	.	.	.	F	C	P	R	.	.	R	P	C	.	.	.	.	
7R-1. 10		238.20	B	.	.	.	.	.	.	.	.	.	.	.	.	.	.	.	.	.	.	.	.	.	.	.	.	.	.	.	.	.	.	.	.	.	.		
7R-1. 14		238.24	A X	P	.	F	C	R	P	.	P	.	R	P	P	.	.	.	.	.	.	F	F	R	F	C	.	F	P	.	R	F	R	C	R	.			
7R-1. 32	238.42	A M	.	.	F	.	.	.	.	P	.	.	.	.	.	.	.	.	.	.	.	.	.	.	.	F	F	P	R	.	R	P	P	.	F	.	.		



1983; Erba, 1988; Bralower et al., 1988). The top of this Subzone is based on a distinct and widely recognized event. Erba (1993) correlated the appearance of *Eprolithus floralis* to the upper lower Aptian *deshayesi* ammonite Zone. Bergen (1994) reported this event near the top of the lower Aptian stratotype at la Bédoule-Station de Cassis in Bed 169.

Additional bioevents can be used to subdivide Subzone CC7b. Bralower et al. (1993) subdivided the equivalent *Chiastozygus litterarius* Zone (NC 6) into two subzones based on the LO of *Conusphaera rothii*; these authors placed the LOs of *Nannoconus steinmannii* and *Retecapsa angustiforata* within their Subzone NC6b. Bralower et al. (1993) also indicated equivalent FOs for *Rhagodiscus angustus* and *Hayesites irregularis*. The order of these two events could not be established among the three mid-Cretaceous sections drilled during Leg 149 because early morphotypes of *Rhagodiscus angustus* are very small and their peripheral outlines transitional to elliptical *Rhagodiscus* species.

*Rhagodiscus angustus* Subzone (CC7b) of the *Chiastozygus litterarius* Zone (CC7)

**Definition.** Interval from the first occurrence of *Eprolithus floralis* to the first occurrence of *Prediscosphaera columnata*.

**Authors.** Thierstein (1971) emended by Manivit et al. (1977).

**Age.** Latest early Aptian to earliest Albian.

**Remarks.** This Subzone was recognized in Holes 897C and 897D. It is equivalent to the *Parhabdololithus angustus* Zone (NC7) of other authors (e.g., Roth, 1978, 1983; Erba, 1988; Bralower et al., 1993). Erba (1988, 1993) and Bralower et al. (1993) placed the appearance of *Prediscosphaera columnata* within the latest Aptian. Our study of upper Aptian sections in the Vocontian Trough (Gargasian and Clansayesian stratotypes and an upper Aptian section near Angles) have yielded only specimens of the elliptical species *Prediscosphaera spinosa*. Thierstein (1971, 1973) also placed the appearance of *Prediscosphaera cretacea* (= *Prediscosphaera columnata*) within the lower Albian.

Bralower et al. (1993) subdivided the equivalent *Parhabdololithus angustus* Zone (NC 7) into three subzones based on successive LO of *Micrantholithus hoschulzii* and FO of *Parhabdololithus achlyostaurion*. These subzones could not be recognized in the study material because these two events are below the FO of *Eprolithus floralis*.

Subzone CC7b is represented by single cores in Hole 897C (62R) and Hole 897D (6R). The FOs of *Prediscosphaera spinosa*, *Corollithion achylosum*, *Corollithion acutum*, and *Corollithion protosignum* accompanied the entry of *Eprolithus floralis* in Hole 897C. Only *Corollithion achylosum* accompanied *E. floralis* in Hole 897D. Bralower et al. (1993) showed the appearance of *Prediscosphaera spinosa* in the uppermost portion (upper Subzone NC7C) of the *Parhabdololithus angustus* Zone, but they reported early Aptian appearances for *Corollithion achylosum* and *Corollithion acutum*.

### Hole 897C

The location of Hole 897C is given in Figure 1 and Table 1. Hole 897C was drilled to investigate the top of the crust within the ocean/continent transition, and the nature of the older sediments beneath the Iberia Abyssal Plain. The majority of the cores recovered Tertiary sediments and nonfossiliferous brown claystones (down to Core 149-897C-61R). The sequence below consists of a short interval of conglomerate with intercalations of dark and yellow claystones (from Samples 149-897C-62R-1, 30 cm through 63R-1, 0 cm) and thick intervals of serpentinized peridotite intercalated between dark greenish gray claystones and breccias (down to Core 149-897C-73R). The average thickness of claystones within the peridotite is about 50 cm, and a few nanofossil-bearing samples were also obtained from isolated

rounded clasts. Several dark, greenish gray claystone intervals are barren of nanofossils. Other intervals contain mixed nanofossil assemblages ranging from highly dissolved and monospecific to highly diverse and moderately well preserved.

The nanofossil assemblages recovered from Hole 897C are given in the range chart of Table 3 and the main marker species are summarized in Figure 3. Samples 149-897C-62R-4, 38 cm, 62R-4, 50 cm, and 62R-4, 60 cm from the yellow claystones lack the Aptian markers, and contain a high percentage of reworked Hauterivian to lower Barremian species as indicated by the presence of *Calcicalathina oblongata*, *Crucellipsis cuvillieri*, rare to common *Nannoconus* spp., and few *Micrantholithus* spp. This indicates that the entire assemblage has been reworked from older sediment, probably deposited in shallower water in the continental shelf area.

Sample 149-897C-62R-CC, 16 cm, is assigned to the upper Aptian *R. angustus* Subzone (CC7b) based on the FOs of *Eprolithus floralis*, *Prediscosphaera spinosa*, *Corollithion achylosum*, *Corollithion acutum*, and *Corollithion protosignum*. An early late Aptian age for this sample is indicated by the additional presence of *Rhagodiscus pseudoangustus* and *Calcicalathina* sp. A (see Bergen, 1994). The interval from Samples 149-897C-63R-1, 1 cm through 66R-1, 10 cm, is placed in the *H. irregularis* Subzone (CC7a) based on the FOs of *Hayesites irregularis* and *Flabellites oblongus* (late morphotype) and on the absence of *Eprolithus floralis*. The FO of *Palaeopontosphaera* sp. 1 and the LO of *Conusphaera rothii* occur in Sample 149-897C-63R-1, 1 cm. The FO of *Rhagodiscus angustus* was found in Sample 149-897C-65R-2, 126 cm; the FO of *Vagalapilla* sp. 2 is in Sample 149-897C-65R-2, 114 cm; and the FO of *Braarudosphaera bigelowii* is in Sample 149-897C-64R-2, 64 cm. Sample 149-897C-70R-3, 26 cm, contains *Rhagodiscus achlyostaurion*, *Zygodiscus elegans*, and *Flabellites oblongus* (early morphotype) and lacks *Hayesites irregularis*. This assemblage indicates the Barremian *Micrantholithus hoschulzii* Zone (CC6).

A hiatus may occur in the middle of the Aptian based on the succession of nanofossil events. No sediments containing the nanofossil assemblages from the interval between the FO of *Eprolithus floralis* and the FO of *Corollithion achylosum* were found.

### Hole 897D

The location for Hole 897D is given on Figure 1 and Table 1. Hole 897D was drilled to complete the lithological sequence of basement rocks and sediments recovered at Hole 897C. As described at Hole 897C, the lithological record was separated into a short upper interval and a thicker lower interval. The short conglomerate sequence (upper interval) occurs from intervals 149-897D-6R-1, 0 cm, through 7R-1, 0 cm, and the olive-gray nanofossil claystone is found from Samples 149-897C-7R-1, 0 cm, through 11R-1, 0 cm. Both intervals contain both barren samples and samples with highly diverse, poorly to moderately well-preserved nanofossil assemblages. A detailed range chart for Hole 897D from Cores 149-897D-6R through 10R is given in Table 4, and a summary of the nanofossil events is presented in Figure 5. No sediments were recovered from Cores 149-897D-11R through 25R.

Sample 149-897D-6R-3, 28 cm is assigned to the *R. angustus* Subzone (CC7b) based on the FOs of *Eprolithus floralis* and *Corollithion achylosum* and the presence of *Rhagodiscus pseudoangustus*. The presence of these species indicates an early late Aptian age. At Hole 897D, the base of the upper Aptian is placed at the level of the FO of *Palaeopontosphaera* sp. 1 in Sample 149-897D-6R-CC, 3 cm. The underlying interval, down to Sample 149-897D-10R-4, 139 cm, is assigned to the lower Aptian *H. irregularis* Subzone (CC7a). This interval contains the FOs of *Rhagodiscus angustus* (Sample 149-897D-10R-4, 91 cm), *Braarudosphaera bigelowii* (Sample 149-897D-10R-3, 141 cm), and *Vagalapilla* sp. 2 and *Hayesites irregularis* (Sample 149-897D-10R-3, 71 cm). The bottom of this interval



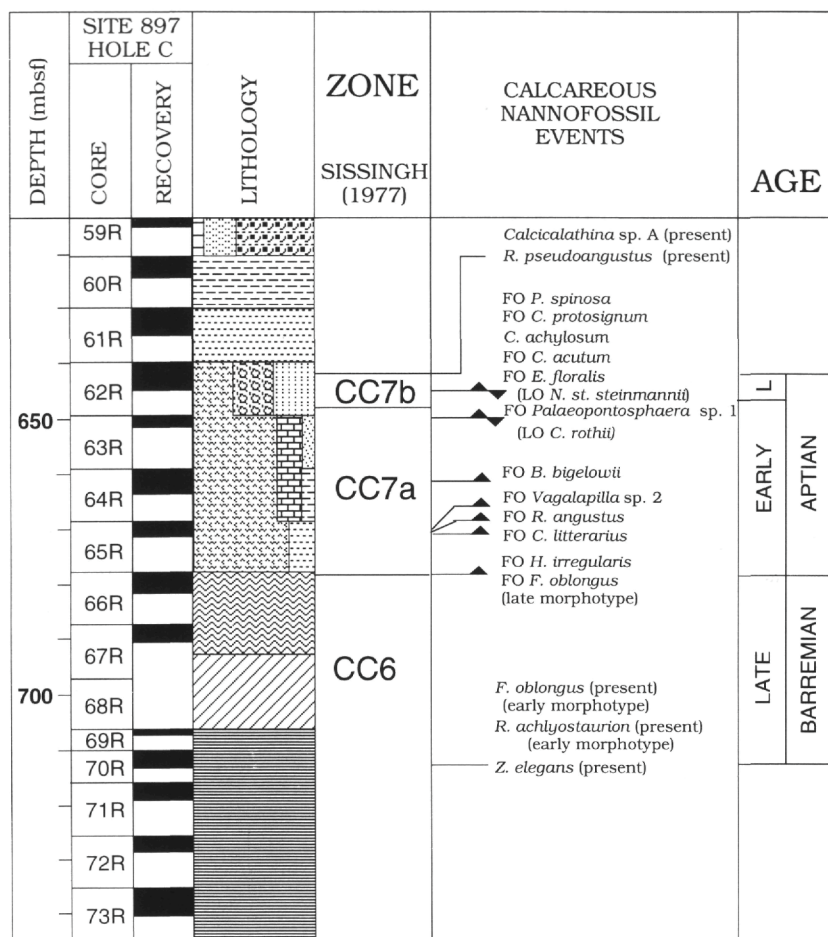


Figure 3. Calcareous nannofossil biostratigraphy of the Cretaceous interval of Hole 897C. Zonal units are modified from Sissingh (1977). The graphic lithology was compiled in Shipboard Scientific Party (1994). See Figure 4 for a summary of the lithologic symbols used in the ODP *Initial Reports* volume.

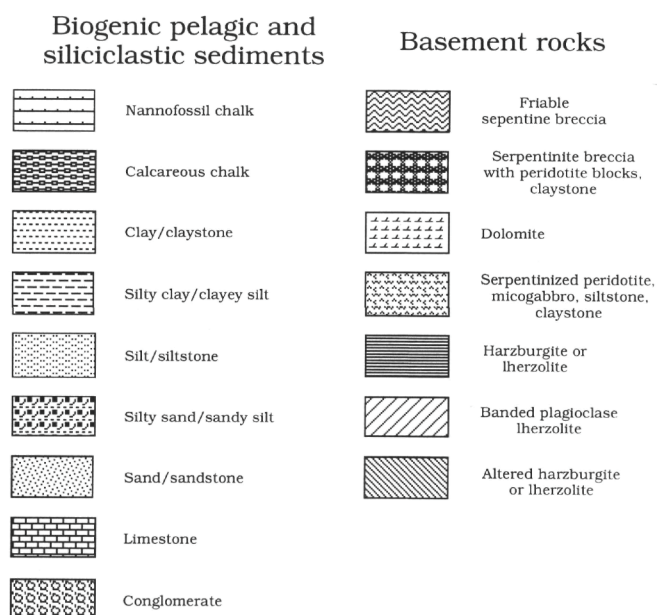


Figure 4. Summary of graphic symbols used in the lithology column in Figures 3, 5, and 6 (only intervals exceeding 20 cm in thickness are shown).

*Hayesites irregularis* below the FO of *R. angustus* found at Hole 899B confirms the placement of the lowermost samples of Hole 897D in the lower Aptian rather than in the uppermost Barremian.

Holes 897C, 897D, and 899B are correlated in Figure 7. The base of the mid-Aptian hiatus is placed below the FO of *E. floralis* (not observed in Hole 899B) and the top is at the FO of *C. achylosum*.

### SUMMARY

A detailed taxonomic and biostratigraphic study was conducted on Tithonian calcareous nannofossils from Hole 901A on the Iberia Abyssal Plain, in the Northeast Atlantic Ocean. Diversity and abundance vary greatly in the Upper Jurassic black shales, which contain early and late Tithonian nannofossil assemblages. The overall diversity of these nannofossil assemblages (more than 100 species) is extremely high, relative to published studies on contemporaneous material. Numerous species thought to have late Tithonian to early Cretaceous appearances are present in these black shales, possibly indicating that a major radiation and turnover in the nannofossil assemblages occurred during the early Tithonian. It is possible that many species originated at high latitudes earlier than has been recognized previously, because of the poor boreal nannofossil record (largely because of unfavorable facies and the limited number of studies). The dominance of radiate placoliths and muroliths (including several species of *Stradnerlithus*) suggest Boreal affinities, although the Tethyan genus *Conusphaera* is also present. The nannofossils assemblages recorded in Tithonian sediments from Site 901 may be explained by the following possibilities:

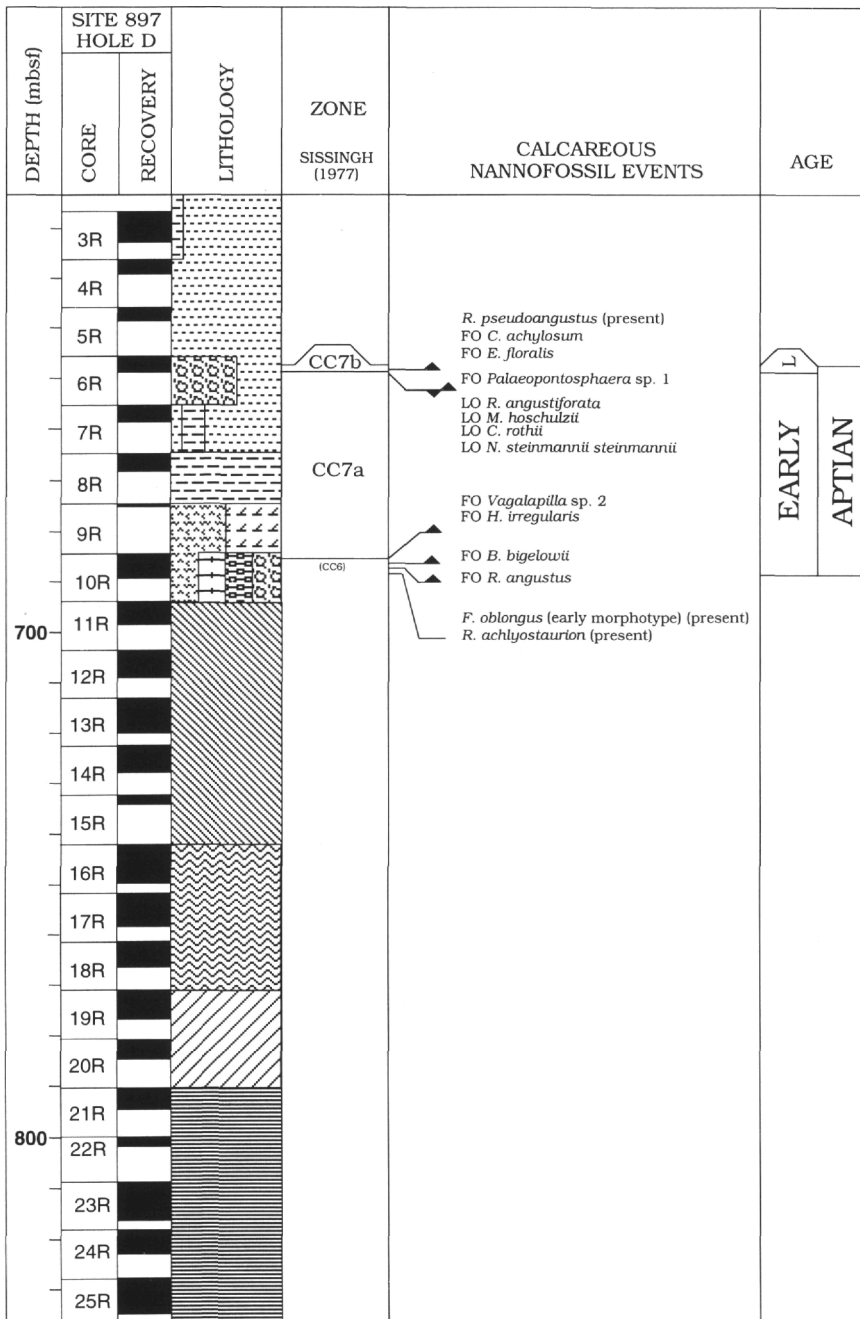


Figure 5. Calcareous nannofossil biostratigraphy of the Cretaceous interval of Hole 897D; see Figure 4 for explanation of lithologic symbols.

1. The mixture of Boreal and Tethyan elements identified at this site may indicate that this site was situated at the southern edge of the boreal province during Tithonian time.
2. The developing North Atlantic rift basin could have created a link to the north to a seaway that existed between the Boreal province and the area of Site 901 and could have controlled the migration of the calcareous nannoplankton.
3. Calcareous nannoplankton are very sensitive to sea level variation, and thus their abundance and diversity directly correlate to ecological and environmental changes (temperature and salinity) and nutrients supplies, that are controlled by global variations of sea-level.

Two sites on the Iberia Abyssal Plain drilled at the zone of transition between oceanic and continental crust (Holes 897C, 897D, and 899B) recovered a variety of sediments interbedded with serpenti-

nized peridotite breccias. Calcareous nannofossil abundance and diversity vary greatly in these sediments, although most assemblages are moderately well preserved. Despite the paucity of sediment, recovered nannofossil assemblages indicate a mid-Aptian hiatus (Fig. 7) between uppermost Barremian/lower Aptian and a thin lower upper Aptian section.

Sediments overlying the upper Barremian/Aptian section consist of conglomerates and brown-red claystone, which are barren of calcareous nannofossils and indicate deposition below the CCD.

#### ACKNOWLEDGMENTS

The study was supported by the Swiss National Science Foundation (Grant 8220-033188). The authors give many thanks to James J. Pospichal for reviewing an early version of this manuscript and J.

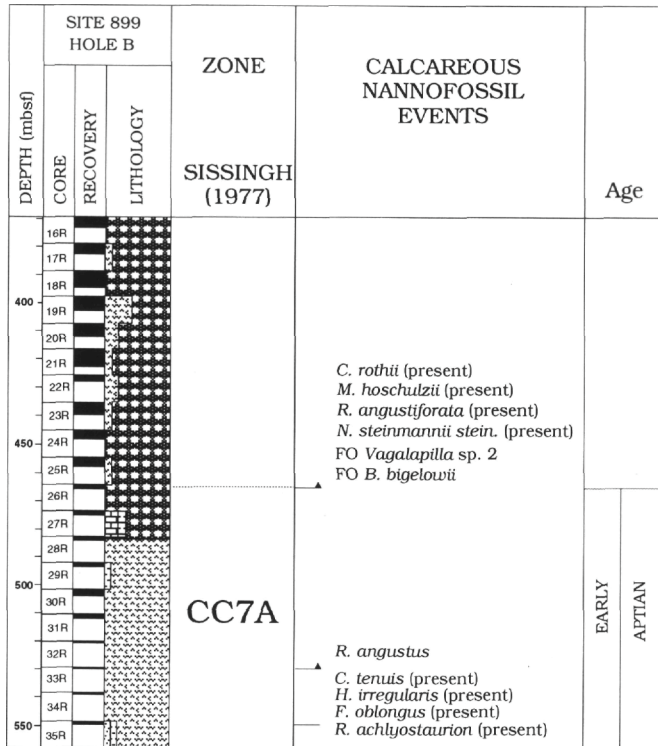


Figure 6. Calcareous nannofossil biostratigraphy of the Cretaceous interval of Hole 899B; see Figure 4 for explanation of lithologic symbols.

Mitchener Covington for providing the BugWare range chart assistance. We thank Kim Riddle for her time and assistance during the work on the scanning electron microscope. We thank E. Erba and J. Crux for the critical review of the manuscript, and E. Kapitan-White for a thorough review that resulted in a much improved paper.

REFERENCES

Applegate, J.L., and Bergen, J.A., 1988. Cretaceous calcareous nannofossil biostratigraphy of sediments recovered from the Galicia Margin, ODP Leg 103. In Boillot, G., Winterer, E.L., et al., *Proc. ODP, Sci. Results*, 103: College Station, TX (Ocean Drilling Program), 293-348.

Bergen, J.A., 1994. Berriasian to early Aptian calcareous nannofossils from the Vocontian Trough (SE France) and Deep Sea Drilling Site 534: new nannofossil taxa and a summary of low-latitude biostratigraphic events. *J. Nannoplankt. Res.*, 16:59-69.

-----, in press. Jurassic calcareous nannofossils from Portugal. *Bull. Am. Paleontol.*

Black, M., 1971. Coccoliths of the Speeton Clay and Sutterby Marl. *Proc. Yorks. Geol. Soc.*, 38:381-424.

-----, 1972. British Lower Cretaceous coccoliths. I. Gault Clay. 1. *Monogr. Palaeontogr. Soc. London*, 126:1-48.

-----, 1973. British Lower Cretaceous coccoliths. I. Gault Clay. 2. *Monogr. Palaeontogr. Soc. London*, 127:49-112.

Black, M., and Barnes, B., 1959. The structure of coccoliths from the English Chalk. *Geol. Mag.*, 96:321-328.

Bown, P.R., and Cooper, M.K.E., 1989a. Conical calcareous nannofossils in the Mesozoic. In Crux, J.A., and van Heck, S.E. (Eds.), *Nannofossils and their Applications*. Brit. Micropalaeontol. Soc. Ser., 98-106.

-----, 1989b. New calcareous nannofossil taxa from the Jurassic. *J. Micropalaeontol.*, 8:91-96.

Bown, P.R., Cooper, M.K.E., and Lord, A.R., 1988. A calcareous nannofossil biozonation scheme for the early to mid Mesozoic. *Newsl. Stratigr.*, 20:91-114.

Bralower, T.J., Monechi, S., and Thierstein, H.R., 1989. Calcareous nannofossil zonation of the Jurassic-Cretaceous boundary interval and correlation with the geomagnetic polarity timescale. *Mar. Micropaleontol.*, 14:153-235.

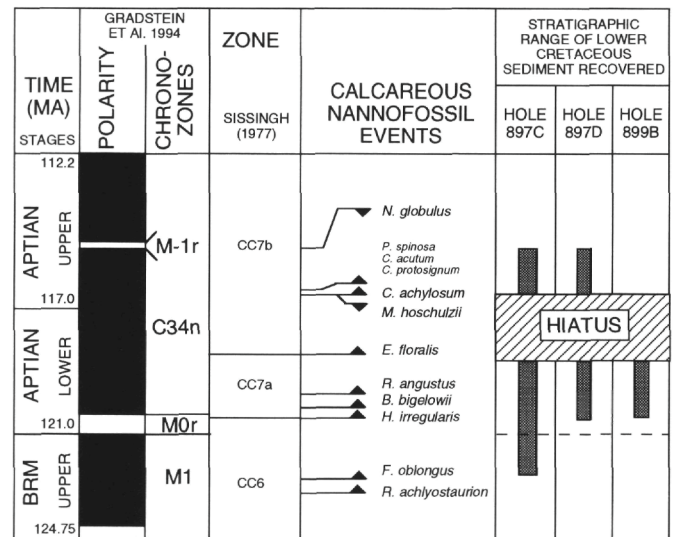


Figure 7. Chronostratigraphy, magnetostratigraphy of Gradstein et al. (1994), zonal units modified from Sissingh (1977), summary of calcareous nannofossil events, and correlation of the Cretaceous interval for Holes 897C, 897D, and 899B.

Bralower, T.J., Sliter, W.V., Arthur, M.A., Leckie, R.M., Allard, D.J., and Schlanger, S.O., 1993. Dysoxic/anoxic episodes in the Aptian-Albian (Early Cretaceous). In Pringle, M.S., Sager, W.W., Sliter, M.V., and Stein, S. (Eds.), *The Mesozoic Pacific: Geology, Tectonics, and Volcanism*. Geophys. Monogr., Am. Geophys. Union, 77:5-37.

Bramlette, M.N., and Martini, E., 1964. The great change in calcareous nannoplankton fossils between the Maestrichtian and Danian. *Micropaleontology*, 10:291-322.

Brönnimann, P., 1955. Microfossils *Incertae sedis* from the Upper Jurassic and Lower Cretaceous of Cuba. *Micropaleontology*, 1:28-51.

Bukry, D., 1969. Upper Cretaceous coccoliths from Texas and Europe. *Univ. Kansas Paleontol. Contrib.*, 51:1-79.

Cepek, P., and Hay, W.W., 1969. Calcareous nannoplankton and biostratigraphic subdivision of the Upper Cretaceous. *Trans. Gulf Coast Assoc. Geol. Soc.*, 19:323-336.

Cooper, M.K.E., 1987. New calcareous nannofossil taxa from the Volgian Stage (Upper Jurassic) leptostratotype site at Gorodishche, U.S.S.R. *Neues Jahrb. Geol. Palaeontol. Mh.* (Stuttgart), 10:606-612.

Covington, J.M., and Wise, S.W., Jr., 1987. Calcareous nannofossil biostratigraphy of a Lower Cretaceous deep-sea fan: Deep Sea Drilling Project Leg 93 Site 603, lower continental rise off Cape Hatteras. In van Hinte, J.E., Wise, S.W., Jr., et al., *Init. Repts. DSDP*, 93: Washington (U.S. Govt. Printing Office), 617-660.

Crux, J.A., 1982. Upper Cretaceous (Cenomanian to Campanian) calcareous nannofossils. In Lord, A.R. (Ed.), *A Stratigraphical Index of Calcareous Nannofossils*. Brit. Micropaleontol. Soc. Ser., 81-135.

-----, 1987. Six new species of calcareous nannofossils from the Lower Cretaceous strata of England and Germany. *INA Newsl.*, 9:30-35.

-----, 1989. Biostratigraphy and paleogeographical applications of Lower Cretaceous nannofossils from north-western Europe. In Crux, J.A., and van Heck, S.E. (Eds.), *Nannofossils and Their Applications*: Chichester (Ellis Horwood), 143-211.

Deflandre, G., 1939. Les stéphanolithes, représentants d'un type nouveau de coccolithes du Jurassique supérieur. *C. R. Acad. Sci Ser. 2*, 208:1331-1333.

-----, 1947. *Braarudosphaera* nov. gen., type d'une famille nouvelle de Coccolithophoridés actuels à éléments composites. *C. R. Acad. Sci. Ser. 2*, 225:439-441.

-----, 1953. Hétérogénéité intrinsèque et pluralité des éléments dans les coccolithes actuels et fossiles. *C. R. Acad. Sci. Ser. 2*, 237:1785-1787.

-----, 1963. Sur les Microrhabdulidés, famille nouvelle des Nannofossils calcaires. *C. R. Acad. Sci. Ser. 2*, 256:3484-3486.

-----, 1939. Les stéphanolithes, représentants d'un type nouveau de coccolithes du Jurassique supérieur. *C. R. Acad. Sci Ser. 2*, 208:1331-1333.

- , 1947. *Braarudosphaera* nov. gen., type d'une famille nouvelle de Coccolithophoridés actuels a éléments composites. *C. R. Acad. Sci. Ser. 2*, 225:439-441.
- , 1953. Hétérogénéité intrinsèque et pluralité des éléments dans les coccolithes actuels et fossiles. *C. R. Acad. Sci. Ser. 2*, 237:1785-1787.
- Deflandre, G., and Pert, C., 1954. Observations sur les coccolithophoridés actuels et fossiles en microscopie ordinaire et électronique. *Ann. Paleontol.*, 40:115-176.
- de Kaenel, E., and Bergen, J.A., 1993. New Early and Middle Jurassic coccolith taxa and biostratigraphy from the eastern proto-Atlantic (Morocco, Portugal, and DSDP Site 574B). *Eclogae Geol. Helv.*, 83:861-907.
- Erba, E., 1988. Aptian-Albian calcareous nannofossil biostratigraphy of the Scisti a Fucoidi cored at Piobbico (Central Italy). *Riv. Ital. Paleontol. Stratigr.*, 94:249-284.
- , 1993. The Early Aptian "nannoconid crisis": a paleobiologic response to global change. *Paleopelagos*, 3:59-73.
- Gartner, S., 1968. Coccoliths and related calcareous nannofossils from Upper Cretaceous deposits of Texas and Arkansas. *Univ. Kansas Paleontol. Contrib.*, 48:1-56.
- Gorka, H., 1957. *Coccolithophoridae* z gornego mastrychtu Polski srod-kowej (Les Coccolithophoridés du Maastrichtien supérieur de Pologne). *Acta Palaeontol. Polon.*, 2:235-284.
- Gradstein, F.M., Agterberg, P.P., Ogg, J.G., Hardenbol, J., van Veen, P., Thierry, J., and Huang, Z., 1994. A Mesozoic time scale. *J. Geophys. Res.*, 99:24051-24074.
- Gran, H.H., and Braarud, T., 1935. A quantitative study of the phytoplankton in the Bay of Fundy and the Gulf of Maine (including observations of the hydrogeology, chemistry and turbidity). *J. Biol. Board Can.*, 1:279-467.
- Grün, W., and Allemann, F., 1975. The Lower Cretaceous of Caravaca (Spain), Berriasian calcareous nannoplankton of the Miravetes Section (subbetic zone, Prov. of Murcia). *Eclogae Geol. Helv.*, 68:147-211.
- Grün, W., Prins, B., and Zweili, F., 1974. Coccolithophoriden aus dem Lias epsilon von Holzmaden (Deutschland). *Neues. Jahrb. Geol. Palaeontol. Abh.*, 147:294-328.
- Grün, W., and Zweili, P., 1980. Das kalkige Nannoplankton der Dogger-Malm-Grenze im Berner Jura bei Liesberg (Schweiz). *Jahrb. Geol. Bundesanst. Austria*, 123:213-341.
- Hill, M.E., 1976. Lower Cretaceous calcareous nannofossils from Texas and Oklahoma. *Paleontographica B*, 156:103-179.
- Jakubowski, M., 1986. New calcareous nannofossil taxa from the Lower Cretaceous of the North Sea. *INA Newsl*, 8:38-42.
- Kamptner, E., 1927. Beitrag zur Kenntnis adriatischer Coccolithophoriden. *Arch. Protistenkd.*, 58:173-184.
- , 1931. *Nannoconus steinmanni* nov. gen., nov. spec., ein merkwürdiges gesteinsbildendes Mikrofossil aus dem jüngeren Mesozoikum der Alpen. *Palaontol. Z.*, 13:288-298.
- Loeblich, A.R., and Tappan, H., 1963. Type fixation and validation of certain calcareous nannoplankton genera. *Proc. Biol. Soc. Wash.*, 76:191-196.
- , 1966. Annotated index and bibliography of the calcareous nannoplankton, I. *Phycologia*, 5:81-216.
- Manivit, H., 1961. Contribution à l'étude des coccolithes de l'Eocène. *Publ. Serv. Carte géol. Algér.*, 2(25):331-382.
- , 1966. Sur quelques coccolithes nouveaux du Neocomien. *C.R. Soc. Geol. Fr.*, 7:267-268.
- , 1971. Nannofossiles calcaires du Crétacé Français (Aptien-Maastrichtien). Essai de biozation appuyée sur les stratotypes [Thèse Doctorate d'Etat]. Fac. Sci. d'Orsay.
- Manivit, H., Perch-Nielsen, K., Prins, B., and Verbeek, J.W., 1977. Mid-Cretaceous calcareous nannofossil biostratigraphy. *Proc. K. Ned. Akad. Wet., Ser. B: Palaeontol., Geol. Phys., Chem.*, 80:169-181.
- Medd, A.W., 1971. Some Middle and Upper Jurassic Coccolithophoridae from England and France. In Farinacci, A. (Ed.), *Proc. 2nd Int. Conf. Planktonic Microfossils Roma 1970*: Rome (Ed. Tecnosci.), 2:821-845.
- , 1979. The Upper Jurassic coccoliths from the Haddenham and Gamlingay boreholes (Cambridgeshire, England). *Eclogae Geol. Helv.*, 72:19-109.
- Noël, D., 1957. Coccolithes des terrains Jurassiques de Algérie. *Publ. Serv. Carte Geol. Algerie*, 2:303-345.
- , 1959. Etude de Coccolithes du Jurassique et Crétacé inférieur. *Bull. Serv. Carte Geol. Algerie*, 2:155-196.
- , 1965. Sur les coccolithes du Jurassique européen et d'Afrique du Nord. Essai de classification des coccolithes fossiles. *Ed. C.N.R.S.*, 1-209.
- , 1973. Nannofossiles calcaires de sédiments Jurassiques finement laminés. *Bull. Mus. Nat. Hist. Nat., Sci. Terre*, 14:95-156.
- Perch-Nielsen, K., 1968. Der Feinbau und die Klassifikation der Coccolithen aus dem Maastrichtien von Dänemark. *Biol. Skr. K. Danske Vidensk.*, 16:1-96.
- , 1984. Validation of new combination. *INA Newsl.*, 6:42-46.
- , 1985. Mesozoic calcareous nannofossils. In Bolli, H.M., Saunders, J.B., and Perch-Nielsen, K. (Eds.), *Plankton Stratigraphy*: Cambridge (Cambridge Univ. Press), 329-426.
- Pienaar, R.N., 1969. Upper Cretaceous coccolithophorids from Zululand, South Africa. *Palaeontology*, 11:361-367.
- Prins, B., 1969. Evolution and stratigraphy of coccolithinids from the Lower and Middle Lias. In Brönnimann, P., and Renz, H.H. (Eds.), *Proc. 1st Int. Conf. Planktonic Microfossils*, Geneva, 2:547-558.
- Reale, V., and Monechi, S., 1994. *Cyclagelosphaera wiedmannii* new species, a marker for the Callovian. *J. Nanno. Res.*, 16:117-119.
- Reinhardt, P., 1964. Einige Kalkflagellaten Gattungen (Coccolithophoriden, Coccolithineen) aus dem Mesozoikum Deutschlands. *Monatsber. Deut. Akad. Wiss. Berlin*, 6:749-759.
- , 1965. Neue Familien für fossile Kalkflagellaten (Coccolithophoriden, Coccolithineen). *Monatsber. Dtsch. Akad. Wiss. Berlin*, 7:30-40.
- , 1966. Zur Taxinomie und Biostratigraphie des fossilen Nannoplanktons aus dem Malm, der Kreide und dem Alttertiar Mitteleuropas. *Freiberg. Forschungsh. C*, 196:1-109.
- , 1967. Fossile Coccolithen mit rhagoidem Zentralfeld (Fam Ahmuellerellaceae, Subord. Coccolithineae). *Neues. Jahrb. Geol. Palaeontol. Monatsh.*, 1967:163-178.
- , 1971. Synopsis der Gattungen und Arten der mesozoischen Coccolithen und anderer kalkiger Nannofossilien. III. *Freiberg. Forschungsh. C* 267:19-41.
- Risatti, J.B., 1973. Nannoplankton biostratigraphy of the Upper Bluffport Marl-Lower Prairie Bluff Chalk interval (Upper Cretaceous), in Mississippi. In Smith, L.A., and Hardenbol, J. (Eds.): *Proc. Symp. Calc. Nannofossils*. Gulf Coast Sect., Soc. Econ. Paleontol. Mineral., 3-57.
- Rood, A.P., Hay, W.W., and Barnard, T., 1971. Electron microscope studies of Oxford clay coccoliths. *Eclogae Geol. Helv.*, 64:245-272.
- , 1973. Electron microscope studies of Lower and Middle Jurassic coccoliths. *Eclogae Geol. Helv.*, 66:365-382.
- Roth, P.H., 1973. Calcareous nannofossils—Leg 17, Deep Sea Drilling Project. In Winterer, E.L., Ewing, J.I., et al., *Init. Repts. DSDP*, 17: Washington (U.S. Govt. Printing Office), 695-795.
- , 1978. Jurassic and Lower Cretaceous nannoplankton biostratigraphy and oceanography of the northwestern Atlantic Ocean. In Benson, W.E., Sheridan, R.E., et al., *Init. Repts. DSDP*, 44: Washington (U.S. Govt. Printing Office), 731-759.
- , 1983. Jurassic and Lower Cretaceous calcareous nannofossils in the western North Atlantic (Site 534): biostratigraphy, preservation, and some observations on biogeography and paleoceanography. In Sheridan, R.E., Gradstein, P.M., et al., *Init. Repts. DSDP*, 76: Washington (U.S. Govt. Printing Office), 587-621.
- Roth, P.H., and Thierstein, H., 1972. Calcareous nannoplankton: Leg 14 of the Deep Sea Drilling Project. In Hayes, D.E., Pimm, A.C., et al., *Init. Repts. DSDP*, 14: Washington (U.S. Govt. Printing Office), 421-485.
- Shipboard Scientific Party, 1994. Site 898. In Sawyer, D.S., Whitmarsh, R.B., Klaus, A., et al., *Proc. ODP, Init. Repts.*, 149: College Station, TX (Ocean Drilling Program), 115-146.
- Sissingh, W., 1977. Biostratigraphy of Cretaceous calcareous nannoplankton. *Geol. Mijnbouw*, 56:37-50.
- , 1978. Microfossil biostratigraphy and stage-stratotypes of the Cretaceous. *Geol. Mijnbouw*, 57:433-440.
- Stover, L.E., 1966. Cretaceous coccoliths and associated nannofossils from France and the Netherlands. *Micropaleontology*, 12:133-167.
- Stradner, H., 1963. New contributions to Mesozoic stratigraphy by means of nannofossils. *Proc. 6th World Petrol. Congr.*, Sect. 1, Pap. 4:1-16.
- Stradner, H., and Adamiker, D., 1966. Nannofossilien aus Bohrkernen und ihre elektronenmikroskopische Bearbeitung. *Erdoel-Erdgas-Z.*, 82:330-341.
- Thierstein, H.R., 1971. Tentative Lower Cretaceous calcareous nannoplankton zonation. *Eclogae Geol. Helv.*, 64:458-488.
- , 1973. Lower Cretaceous calcareous nannoplankton biostratigraphy. *Abh. Geol. Bundesanst. (Austria)*, 29:1-52.
- , 1975. Calcareous nannoplankton biostratigraphy at the Jurassic-Cretaceous boundary. Colloque sur la limite Jurassique-Crétacé, Lyon, Neuchâtel, Sept. 1973. *Mem. B.R.G.M.*, 86:84-94.

- Trejo, M., 1969. *Conusphaera mexicana*, un nuevo coccolitoforido del Jurásico superior de México. *Rev. Inst. Mexicano Petrol.*, 1:5-15.
- Varol, O., and Girgis, M.H., 1994. New taxa and taxonomy of some Jurassic to Cretaceous calcareous nannofossils. *Neues. Jahrb. Geol. Palaeontol. Abh.*, 192:221-253.
- Verbeek, J.W., 1977. Calcareous nannoplankton biostratigraphy of middle and upper Cretaceous deposits in Tunisia, southern Spain and France. *Utrecht Micropaleontol. Bull.*, 16:1-157.
- Wilcoxon, J.A., 1972. Upper Jurassic-Lower Cretaceous calcareous nannoplankton from the Western North Atlantic Basin. In Hollister, C.D., Ewing, J.I., et al., *Init. Repts. DSDP*, 11: Washington (U.S. Govt. Printing Office), 427-457.
- Wind, F.H., 1978. Western North Atlantic Upper Jurassic calcareous nannofossil biostratigraphy. In Benson, W.E., Sheridan, R.E., et al., *Init. Repts. DSDP*, 44: Washington (U.S. Govt. Printing Office), 761-773.
- Wind, F.H., and Cepek, P., 1979. Lower Cretaceous calcareous nannoplankton from DSDP Hole 397A (Northwest African Margin). In von Rad, U., Ryan, W.B.F., et al., *Init. Repts. DSDP*, 47: Washington (U.S. Govt. Printing Office), 241-255.
- Wise, S.W., Jr., 1983. Mesozoic and Cenozoic calcareous nannofossils recovered by Deep Sea Drilling Project Leg 71 in the Falkland Plateau region, Southwest Atlantic Ocean. In Ludwig, W.J., Krashenninikov, V.A., et al., *Init. Repts. DSDP*, 71 (Pt. 2): Washington (U.S. Govt. Printing Office), 481-550.
- Wise, S.W., Jr., and Wind, F.H., 1977. Mesozoic and Cenozoic calcareous nannofossils recovered by DSDP Leg 36 drilling on the Falkland Plateau, Southwest Atlantic sector of the Southern Ocean. In Barker, P.P., Dalziel, I.W.D., et al., *Init. Repts. DSDP*, 36: Washington (U.S. Govt. Printing Office), 269-492.
- Worsley, T., 1971. Calcareous nannofossil zonation of Upper Jurassic and Lower Cretaceous sediments from the Western Atlantic. In Farinacci, A. (Ed.), *Proc. 2nd Planktonic Conf. Roma*, 2:1301-1322.

**Date of initial receipt: 6 December 1994**

**Date of acceptance: 20 June 1995**

**Ms 149SR-206**





Table 5. Stratigraphic distribution of calcareous nannofossil taxa from Hole 897B.

Age	Zone	Core, section, interval (cm)	Depth (mbsf)	Abundance	Preservation	<i>Assipetra infracretacea</i>	<i>Assipetra terebrodentarius</i>	<i>Biscutum rotatorium</i>	<i>Braarudosphaera bigelowii</i>	<i>Calciatathina</i> sp. A	<i>Chitaozgyus tenuis</i>	<i>Conusphaera mexicana mexicana</i>	<i>Conusphaera mexicana minor</i>	<i>Conusphaera rothii</i>	<i>Crucellipsis cuvillieri</i>	<i>Cyclagelosphaera margerelii</i>	<i>Diadorhombus rectus</i>	<i>Diazomatolithus lehmannii</i>	<i>Ellipsogelosphaera britannica</i>	<i>Flabellites oblongus</i>	<i>Hayesites irregularis</i>	<i>Hexapodorhabdus cuvillieri</i>	<i>Lithraphidites camiolensis</i>	<i>Lucianorhabdus salomontii</i>	<i>Maniuteila pennaioidea</i>	<i>Markalius circumradiatus</i>	<i>Markalius ellipticus</i>	<i>Micrantholithus hoschulzii</i>	<i>Micrantholithus obtusus</i>	<i>Micrantholithus chiastus</i>							
early Aptian	CC7A	26R-1, 85-86	465.01	A X	P R R P R	.	.	.	.	.	.	R P R P	.	.	.	R . R P	.	.	.	P P F	.	R	.	.	.	.	.	.	.	.	.						
		26R-2, 0-6	465.64	B	.	.	.	.	.	.	.	.	.	.	.	.	.	.	.	.	.	.	.	.	.	.	.	.	.	.	.	.					
		27R-1, 65-66	474.01	C M	.	R .	.	.	R	.	.	.	.	.	.	.	.	P	.	.	.	.	P	.	.	.	.	.	.	P	.	P					
		27R-1, 97-98	474.57	F P	.	.	.	.	.	.	.	.	.	.	.	.	.	.	.	.	.	.	.	.	.	.	.	.	.	.	.	.	.				
		28R-1, 132-133	484.19	C P	R .	.	.	.	.	.	.	.	.	.	.	.	R	.	.	R	.	.	F	.	P	P	.	.	.	.	P	.					
		29R-1, 21-22	480.11	A M	.	R .	.	.	.	.	.	P P	.	.	.	.	.	.	.	.	.	.	F P	.	.	.	.	.	.	.	.	.	.				
		29R-1, 89-91	492.99	B	.	.	.	.	.	.	.	.	.	.	.	.	.	.	.	.	.	.	.	.	.	.	.	.	.	.	.	.	.				
		29R-2, 0-7	493.54	B	.	.	.	.	.	.	.	.	.	.	.	.	.	.	.	.	.	.	.	.	.	.	.	.	.	.	.	.	.	.			
		31R-1, 0-9	510.50	B	.	.	.	.	.	.	.	.	.	.	.	.	.	.	.	.	.	.	.	.	.	.	.	.	.	.	.	.	.	.			
		32R-1, 5-6	520.05	F P	.	.	.	.	.	.	.	.	.	.	.	.	.	.	.	.	.	.	.	.	.	.	.	.	.	.	.	.	.	.	.		
		32R-1, 35-36	520.40	B	.	.	.	.	.	.	.	.	.	.	.	.	.	.	.	.	.	.	.	.	.	.	.	.	.	.	.	.	.	.	.	.	
		33R-1, 12-15	529.62	F P	R P	.	.	.	.	.	.	.	.	.	.	.	.	.	.	.	.	.	.	.	.	.	.	.	.	.	.	.	.	.	.	.	
		33R-1, 15-16	529.67	B	.	.	.	.	.	.	.	.	.	.	.	.	.	.	.	.	.	.	.	.	.	.	.	.	.	.	.	.	.	.	.	.	.
		33R-1, 99-100	549.38	A M	R F	.	.	R	.	R	R P P R R	.	.	.	.	.	.	.	.	.	R	.	P	F	.	.	.	R R R R	.	.	.	.	.	.	.		
		35R-1, 118-120	549.58	B	.	.	.	.	.	.	.	.	.	.	.	.	.	.	.	.	.	.	.	.	.	.	.	.	.	.	.	.	.	.	.	.	.
		37R-1, 22-26	557.82	B	.	.	.	.	.	.	.	.	.	.	.	.	.	.	.	.	.	.	.	.	.	.	.	.	.	.	.	.	.	.	.	.	.

Age	Zone	Core, section, interval (cm)	Depth (mbsf)	Abundance	Preservation	<i>Microstaurius quadratus</i>	<i>Nannoconus bermudezi</i>	<i>Nannoconus globulus</i>	<i>Nannoconus kamptneri kamptneri</i>	<i>Nannoconus ligius</i>	<i>Nannoconus steinmannii steinmannii</i>	<i>Palaeopontosphaera salebrosa</i>	<i>Percivalia fenestrata</i>	<i>Reinhardtites scutula</i>	<i>Retecapsa angustiforata</i>	<i>Rhagodiscus achlyostaurion</i>	<i>Rhagodiscus angustus</i>	<i>Rhagodiscus asper</i>	<i>Rhagodiscus pseudoangustus</i>	<i>Rotelapillus laffitei</i>	<i>Speetonia colligata</i>	<i>Tubodiscus jurapelagicus</i>	<i>Vagalapilla</i> sp. 1	<i>Watznaueria barnesae</i>	<i>Watznaueria biporta</i>	<i>Watznaueria fossacincta</i>	<i>Zeugrhabdotus embergeri</i>	<i>Zeugrhabdotus erectus</i>	<i>Zeugrhabdotus trirectis</i>	<i>Zygodiscus xenotus</i>	<i>Zygodiscus elegans</i>							
early Aptian	CC7A	26R-1, 85-86	465.01	A X	F . F . R	R R R R R	.	.	.	.	R R R R R	.	.	.	.	R C P	.	.	.	.	P P C R	.	F R	.	.	.	R F P R R	.	.	.	.	.						
		26R-2, 0-6	465.64	B	.	.	.	.	.	.	.	.	.	.	.	.	.	.	.	.	.	.	.	.	.	.	.	.	.	.	.	.	.	.	.	.	.	
		27R-1, 65-66	474.01	C M	R .	.	.	.	.	.	.	.	.	.	.	.	.	F	.	.	.	.	.	F R	.	.	.	.	.	.	.	.	.	.	.	.		
		27R-1, 97-98	474.57	F P	.	.	.	.	.	.	R	.	.	.	.	.	.	R	.	.	.	.	.	.	F	.	.	.	.	.	.	.	.	.	.	.	.	
		28R-1, 132-133	484.19	C P	F .	.	.	.	.	.	.	.	R R	.	.	.	.	F	.	.	.	.	.	.	C	.	R	.	.	.	.	.	.	.	.	.		
		29R-1, 21-22	480.11	A M	C .	.	.	.	.	.	.	.	.	.	.	R	.	C	.	.	.	.	.	.	C	.	R	.	.	.	.	.	.	.	.	.		
		29R-1, 89-91	492.99	B	.	.	.	.	.	.	.	.	.	.	.	.	.	.	.	.	.	.	.	.	.	.	.	.	.	.	.	.	.	.	.	.	.	
		29R-2, 0-7	493.54	B	.	.	.	.	.	.	.	.	.	.	.	.	.	.	.	.	.	.	.	.	.	.	.	.	.	.	.	.	.	.	.	.	.	
		31R-1, 0-9	510.50	B	.	.	.	.	.	.	.	.	.	.	.	.	.	.	.	.	.	.	.	.	.	.	.	.	.	.	.	.	.	.	.	.	.	.
		32R-1, 5-6	520.05	F P	.	.	.	.	.	.	.	.	.	.	.	.	.	P	.	.	.	.	.	.	F	.	R	.	.	.	.	.	.	.	.	.	.	
		32R-1, 35-36	520.40	B	.	.	.	.	.	.	.	.	.	.	.	.	.	.	.	.	.	.	.	.	.	.	.	.	.	.	.	.	.	.	.	.	.	.
		33R-1, 12-15	529.62	F P	.	.	.	.	.	.	.	.	.	.	.	.	.	R R	.	.	.	.	.	.	F P	.	.	.	.	.	.	.	.	.	.	.	.	.
		33R-1, 15-16	529.67	B	.	.	.	.	.	.	.	.	.	.	.	.	.	.	.	.	.	.	.	.	.	.	.	.	.	.	.	.	.	.	.	.	.	.
		33R-1, 99-100	549.38	A M	R F R F R	C . R R R R	R . F . R	P .	.	.	.	.	.	.	.	.	P	.	.	.	.	.	.	C P	.	R R R	.	.	.	.	.	.	.	.	.	.	.	
		35R-1, 118-120	549.58	B	.	.	.	.	.	.	.	.	.	.	.	.	.	.	.	.	.	.	.	.	.	.	.	.	.	.	.	.	.	.	.	.	.	.
		37R-1, 22-26	557.82	B	.	.	.	.	.	.	.	.	.	.	.	.	.	.	.	.	.	.	.	.	.	.	.	.	.	.	.	.	.	.	.	.	.	.

## APPENDIX A

## Systematics

The following systematic descriptions and discussion include only a portion of the Mesozoic species found during this study. Taxa not cited in Appendix A appear in Appendix B.

Size ranges are as observed in this study with the holotype measurement indicated in parentheses. Photographic negatives are used as types, and film and frame numbers cited herein are stored at the Department of Geology of the Florida State University (FSU). Holotype micrograph numbers are given in the plate captions.

Genus *ANSULASPHAERA* Grün and Zweili, 1980

*Ansulasphaera covingtonii* sp. nov.  
(Pl. 1, Figs. 1-18)

**Diagnosis.** A small- to medium-sized, circular to elliptical species of *Ansulasphaera* with a distally extended element cycle.

**Description.** The circular to elliptical placolith is constructed of three shields. A narrow distal shield is constructed of a single cycle of vertical to subvertical elements. The broad, subhorizontal median shield is constructed of imbricated elements having nonradial sutures. The proximal shield is formed by a single cycle of subvertical, blocky elements. The distal shield height is approximately one-third of the proximal shield height. The central area is open.

In cross-polarized light, this species is easily distinguished in lateral view. In plan view, both the proximal and distal cycles exhibit a first-order white birefringence, whereas the median cycle is faintly birefringent to dark. The proximal element cycle can be distinguished from the distal element cycle by its greater thickness and height.

**Size.** 4.0 to 6.0 (holotype: 4.6  $\mu$ m).

**Remarks.** *Ansulasphaera covingtonii* differs from *Ansulasphaera helvetica* by its distally extended element cycle and younger stratigraphic occurrence. *A. covingtonii* is described herein from the Tithonian and may range into the Cretaceous, whereas *A. helvetica* is not known to have survived the Callovian.

**Derivation of name.** In honor of the nannofossil paleontologist James Mitchener Covington.

**Holotype.** Plate 1, Figures 4-8, specimen transferred from the LM to the SEM.

**Type locality.** ODP Site 901, Iberia Abyssal Plain.

**Type level.** ODP Sample 149-901A-5R-1, 31 cm; Tithonian.

**Occurrence.** Rare to common in Tithonian sediments from ODP Hole 901A.

Genus *AXOPODORHABDUS* Wind and Wise in Wise and Wind, 1977

*Axopodorhabdus cylindratus* (Noël, 1965) Wind and Wise  
in Wise and Wind, 1977  
(Pl. 11, Figs. 3, 10, 11)

*Axopodorhabdus rahla* (Noël, 1965) Grün and Zweili, 1980  
(Pl. 11, Figs. 14, 15)

Genus *BISCUTUM* Black 1959 emended de Kaenel and Bergen, 1993

*Biscutum rotatorium* (Bukry, 1969) comb. nov.

*Bidiscus rotatorius* Bukry, 1969, p. 27, pl. 27, figs. 5-9.

*Discorhabdus rotatorius* (Bukry, 1969) Thierstein, 1973, p. 42, pl. 5, figs. 13-16.

**Remarks.** This species is transferred into the genus *Biscutum* based on its rim construction (i.e., two subhorizontal, unicyclic shields). The central area is imperforate. In cross-polarized light, the distal and proximal shields exhibit a faint birefringence. The central area elements are birefringent.

Genus *BRAARUDOSPHERA* Deflandre, 1947

*Braarudosphaera regularis* Black, 1973  
(Pl. 11, Figs. 26, 27)

Genus *CALCIVASCULARIS* Wiegand, 1984

*Calcivascularis* sp. 1  
(Pl. 6, Figs. 17 and 18)

**Remarks.** This small form of *Calcivascularis* has two sub-parallel walls and a circular horizontal outline. The central portion is filled by cycles of radial elements. This form is present in Kimmeridgian strata in Portugal, south-eastern France, and at DSDP Site 534.

This form is distinguished from *Calcivascularis jansae* Wiegand, 1984 by its small size, continuous central core (in lateral view), and higher number of rim elements.

Genus *CHIASTOZYGUS* Gartner, 1968

*Chiastozygus leptostaurus* Cooper, 1987  
(PL 10, Figs. 13, 14)

Genus *CLEPSILITHUS* Crux, 1987

*Clepsilithus meniscus* sp. nov.  
(Pl. 7, Figs. 6, 14-16)

**Diagnosis.** A very small species of *Clepsilithus* with a narrow rim.

**Description.** A very small, elliptical murolith with a narrow rim. The low distal shield is constructed of imbricated elements. Numerous, somewhat radial elements fused into a central plate extend from the reduced proximal shield toward the center of the coccolith, but leave a small central opening. The rim extinction pattern is unicyclic and weakly birefringent, whereas the central plate is more birefringent.

**Size.** 2.5 to 3.5  $\mu$ m (holotype: 3.0  $\mu$ m).

**Differentiation.** The appearance of a fused central plate composed of thickened, radial bars may be a preservational artifact. The elliptical outline, central opening, and disposition of these central bars conforms to *Clepsilithus* Crux, 1987. It is distinguished from *Clepsilithus polystreptus* by its narrow rim and central plate.

**Derivation of name.** From Greek, *meniskos*: crescent.

**Holotype.** Plate 7, Figures 6, 14-16; specimen transferred from the LM to the SEM.

**Type locality.** ODP Site 901, Iberia Abyssal Plain.

**Type level.** ODP Sample 149-901A-5R-1, 31 cm; Tithonian.

**Occurrence.** Rare in lower Tithonian sediments from ODP Hole 901 A.

Genus *CONUSPHAERA* Trejo, 1969

*Conusphaera mexicana* Trejo, 1969 subsp. *minor* Bralower 1989  
(Pl. 4, Figs. 1-12, 15-17; Pl. 5, Figs. 4, 10; Pl. 6, Figs. 1, 2, 4, 5, 7-13)

*Conusphaera mexicana* Trejo, 1969 subsp. *minor* Bralower ex Bown and Cooper, 1989b; in Bralower, Monechi, and Thierstein, 1989, p. 223, 225, 228, pl. 7, figs. 21-25.

**Remarks.** Rare forms of *Conusphaera mexicana* ssp. *minor* have an extended wall or a low inner core (Pl. 4, Figs. 1 and 4; Pl. 5, Figs. 4 and 10). These specimens are gradational between *Conusphaera sinespina* (elliptical, no inner core) and more typical *C. mexicana* ssp. *minor* (elevated inner core). *C. mexicana* may have evolved from an elliptical murolith with a nonimbricated wall, such as *Stradnerlithus*. Many specimens of *C. mexicana* ssp. *minor* possess an elliptical to subelliptical shape (Pl. 4, Figs. 13 and 14). *C. mexicana* ssp. *minor* is subdivided in this study according to the nannolith shape in plan view (perpendicular to the longitudinal axis) and indicated as *C. mexicana minor* (circular) and *C. mexicana minor* (elliptical) in the Table 2. The abundance of specimens with elliptical or circular apical outline is indicated in Table 2. Both nannolith shapes are present in most nannofossil assemblages. Elliptical specimens are as abundant as circular ones.

Rare detached spines of *C. mexicana* ssp. *minor* were also observed (Pl. 5, Figs 11-17). In cross-polarized light, these forms are similar to small *Polycostella beckmannii*. A specimen transferred during the current study (Plate 5, Figs. 11, 12, 17) show similarities to the holotype of *Polycostella beckmannii* Thierstein, 1971 (pl. 2, fig. 6). Therefore, it is possible that *Polycostella beckmannii* and *Conusphaera mexicana* are related or possibly synonymous. Additional upper Tithonian specimens must be transferred to clarify this potential taxonomic problem.

*Conusphaera mexicana* Trejo, 1969 ssp. *mexicana* (Bralower, 1989)  
(Pl. 6, Figs. 3, 6, 14-16)

*Conusphaera mexicana* Trejo, 1969, p. 6, pl. 1, figs. 1-5; pl. 2, figs. 208, pl. 3, figs. 1-7; pl. 4, figs. 1-4.

*Conusphaera mexicana* Trejo, 1969 subsp. *mexicana* Bralower; in Bralower, Monechi, and Thierstein, 1989, p. 228, pl. 7, figs. 16-20.

**Remarks.** The autonym was fixed by the description of *Conusphaera mexicana* ssp. *minor* by Bralower (in Bralower, Monechi, and Thierstein, 1989). *Conusphaera mexicana* ssp. *mexicana* is distinguished by its greater size and height/width ratio.

*Conusphaera sinespina* sp. nov.  
(Pl. 5, Figs. 1-3, 5-9)

**Diagnosis.** A species of *Conusphaera* with an elliptical horizontal peripheral outline, a low shield, and no central spine (or core).

**Description.** A truncated, conical murolith with an elliptical, horizontal peripheral outline. The low distal shield is formed by a single cycle of 18 to 24 vertical elements, which are oriented with their broad faces tangential to the horizontal periphery. A subhorizontal, proximal element cycle closes the central area; it is constructed of 14 to 16 helical elements that are twisted clockwise (in proximal view).

In plan view, the rim is faintly birefringent and the central, proximal elements are slightly birefringent to dark.

**Size.** 3.0 to 4.0  $\mu\text{m}$  (holotype: 3.4  $\mu\text{m}$ )

**Differentiation.** *Conusphaera sinespina* differs from *Conusphaera mexicana* by its distinct elliptical outline and the absence of an inner central core. In plan view and in cross-polarized light, the central area of *Conusphaera sinespina* exhibits a faint birefringent. The central core of *Conusphaera mexicana* exhibits a first-order white birefringence.

**Derivation of name.** From Latin, *sine*, without, and *spina*, spine.

**Holotype.** Plate 5, Figures 3, 9.

**Type locality.** ODP Site 901, Iberia Abyssal Plain.

**Type level.** ODP Sample 149-901A-5R-1, 31 cm; Tithonian

**Occurrence.** Rare in Tithonian of ODP Hole 901 A.

Genus *CREPIDOLITHUS* Noël 1965

*Crepidolithus parvulus* sp. nov.  
(Pl. 7, Figs. 2, 3, 5, 9-13)

**Diagnosis.** A very small species of *Crepidolithus* with a broad rim and a small central opening spanned by a thin plate.

**Description.** A very small, elliptical murolith with a broad, thick distal shield constructed of 20-24 lath-shaped, imbricated elements. A thin proximal plate fills the central area, but is easily damaged because of its delicate nature. A distal projection is not present.

The rim is faintly birefringent and the central plate is dark in cross-polarized light.

**Size.** 2.5 to 3.5  $\mu\text{m}$  (holotype: 2.8  $\mu\text{m}$ )

**Differentiation.** *Crepidolithus parvulus* differs from other *Crepidolithus* by its extremely small size and younger stratigraphic occurrence.

**Derivation of name.** From Latin, *parvulus*: little.

**Holotype.** Plate 7, Figures 2, 5, 9, 10; specimen transferred from the LM to the SEM.

**Type locality.** ODP Site 901, Iberia Abyssal Plain.

**Type level.** ODP Sample 149-901A-5R-1, 31 cm; Tithonian

**Occurrence.** Rare to few in Tithonian sediments from ODP Hole 901 A.

Genus *CRETARHABDUS* Bramlette and Martini, 1964

*Cretarhabdus conicus* Bramlette and Martini, 1964  
(Pl. 8, Figs. 24, 25)

Genus *CYCLAGELOSPHAERA* Noël, 1965

*Cyclagelosphaera deflandrei* Manivit, 1966

**Remarks.** One morphotype (A) of *Cyclagelosphaera deflandrei* exhibits a yellow birefringence and is identified by its small, circular to subelliptical central area. Although rare in Tithonian sediments from Hole 901 A, this morphotype is more abundant and occurs more consistently than the second morphotype (B). The latter exhibits first-order yellow to red birefringence color

and is identified by its large, elliptical central area. This form is very rare in Tithonian sediments from Hole 901 A.

Genus *DIADORHOMBUS* Worsley, 1971

*Diadorhombus scutulatus* (Medd, 1971) Medd, 1979  
(Pl. 9, Figs. 12, 13)

Genus *DIAZOMATOLITHUS* Noël, 1965

*Diazomatolithus galicianus* sp. nov.  
(Pl. 2, Figs. 1-8; Pl. 3, Figs. 1, 2)

**Diagnosis.** A small- to medium-sized species of *Diazomatolithus* possessing a narrow rim and bicyclic distal shield.

**Description.** The circular placolith is composed of two narrow shields of equal width. The distal shield is bicyclic. Its inner cycle is formed of steeply inclined, radial elements. The slightly broader outer distal cycle is constructed of subhorizontal elements with subradial sutures. The unicyclic proximal shield is constructed of slightly imbricated elements showing some proximal extension. The two shields form an angle of about 50°. The central area is open.

**Size.** 4.0 to 5.5  $\mu\text{m}$  (holotype: 4.3  $\mu\text{m}$ ).

**Remarks.** *Diazomatolithus galicianus* differs from *Diazomatolithus lehmanii* by having a narrower rim composed by two equal-sized shields and a distinct inner distal cycle. *Diazomatolithus* shows its closest morphologic affinities to *Ansulasphaera*.

**Derivation of name.** After the Galicia Margin, off the coast of Portugal.

**Holotype.** Plate 2, Figures 1, 2, 4, 5; specimen transferred from the LM to the SEM.

**Type locality.** ODP Site 901, Iberia Abyssal Plain.

**Type level.** ODP Sample 149-901A-5R-1, 31 cm; Tithonian

**Occurrence.** Present to few in Tithonian sediments from ODP Hole 901 A.

*Diazomatolithus lehmanii* Noël, 1965  
(Pl. 2, Figs. 9-11; Pl. 3, Figs. 3-8)

*Diazomatolithus lehmanii* Noël, 1965 (partim), p. 96, pl. 6, figs. 6(?), 8, 9(?), text fig. 26 (non pl. 6, figs. 7, 10; text figs. 25, 27).

**Remarks.** The problems with the identification of this species result from the composite of forms illustrated as this species by Noël (1965). These specimens belong to the genus *Triscutum* (Noël, 1965, side view, pl. 6, figs. 7, 10; text fig. 25) and possibly specimens of *Discorhabdus* with missing or broken stems (Noël, 1965, pl. 6, figs. 6, 9). Specimens illustrated herein include both a transferred specimen (Pl. 3, Figs. 3-6), as well as a rotated specimen (Pl. 3, Figs. 7, 8) that is nearly identical to the holotype (Noël 1965, pl. 6, fig. 8).

The holotype and specimens illustrated herein characterize *Diazomatolithus lehmanii* as a circular placolith constructed of two relatively broad shields. Elements of both shields are slightly imbricated and surround a large central opening. The proximal shield (orientation is given from the curvature in Pl. 3, Fig. 6) is slightly broader, more steeply inclined, and its elements more strongly curved than the subhorizontal distal shield. A narrow distal wall is also visible (Pl. 3, Figs. 7, 8).

Genus *DUPLEXIPODORHABDUS* Varol and Girgis, 1994

*Duplexipodorhabdus plethotretus* (Wind and Cepeck, 1979) Varol and Girgis, 1994  
(Pl. 11, Figs. 16, 18)

Genus *ETHMORHABDUS* Noël, 1965

*Ethmorhabdus gallicus* Noël, 1965  
(Pl. 11, Figs. 22, 23)

*Ethmorhabdus hauterivianus* (Black, 1971) Applegate, Covington, and Wise in Covington and Wise, 1987  
(Pl. 11, Figs. 24, 25)

*Ethmorhabdus rimosus* Grün and Zweili, 1980  
(Pl. 11, Figs. 20, 21)

*Ethmorhabdus* sp. 1

**Remarks.** This small form of *Ethmorhabdus* has three cycles of small perforations. It differs from *Ethmorhabdus gallicus* (two cycles of perforations) by being smaller and by having fewer perforations arranged in three cycles.

Genus *FLABELLITES* Thierstein, 1973

*Flabellites oblongus* (Bukry, 1969) Crux, 1982

*Watznaueria oblonga* Bukry, 1969, p. 33, pl. 11, figs. 11-12.  
*Flabellites biforaminitis* Thierstein, 1973, p. 41, pl. 5, figs. 1-12.  
*Flabellites oblonga* (Bukry, 1969) Crux, 1982, p. 110, pl. 5.1, fig. 11; pl. 5.8, fig. 1.

**Remarks.** Early morphotypes of *Flabellites oblongus* were observed in the upper Barremian to basal Aptian of ODP Hole 897C. These specimens differ from typical *Flabellites oblongus* by their reduced flanges and higher bar angles.

Genus *GRANTARHABDUS* Black, 1971

*Grantarhabdus bukryi* Black, 1972  
(Pl. 8, Figs. 22, 23)

Genus *HEXAPODORHABDUS* Noël, 1965

*Hexapodorhabdus cuvillieri* Noël, 1965  
(Pl. 11, Figs. 1,2,4-7)

Genus *MARKALIUS* Bramlette and Martini, 1964

*Markalius ellipticus* Grün in Grün and Allemann, 1975  
(Pl. 10, Figs. 1,2,4-7)

Genus *MICROSTAVURUS* Black, 1971

*Microstaurus chiastus* (Worsley, 1971) Grün in Grün and Allemann, 1975  
(Pl. 8, Figs. 20, 21)

Genus *MIRAVETESINA* Grün in Grün and Allemann, 1975

*Miravetesina favula* Grün in Grün and Allemann, 1975  
(Pl. 8, Figs. 26, 27)

Genus *NODOSELLA* Prins, 1969 ex Rood, Hay, and Barnard, 1973

*Nodosella* cf. *N. silvaradion* (Filewicz et al. in Wise and Wind, 1977) Perch-Nielsen, 1984

**Remarks.** This form has a broad rim and a wide central area. It differs from typical *Nodosella silvaradion* by the absence of a central spine. The high number of bars forming a central platform and its thicker rim distinguish it from *Stradnerlithus* species. This form is very rare in lower Tithonian sediments from Hole 901 A.

Genus *OCTOPODORHABDUS* Noël, 1965

*Octopodorhabdus praevisus* Noël, 1965  
(Pl. 11, Figs. 8, 9)

*Octopodorhabdus praevisus* Noël, 1965, p. 107, text fig. 31.

**Remarks.** The type specimen illustration of *Octopodorhabdus praevisus* is a hand drawing of a specimen with eight central perforations; two of these perforations fall in the longitudinal axis of the ellipse. However, the diagnosis of *Octopodorhabdus praevisus* (Noël, 1965, p. 107) indicates that the bars are aligned with the ellipse axes. Specimens attributed to *Octopodorhabdus praevisus* in the current study conform to the hand illustration of the holotype. Six large perforations are always clearly identifiable, whereas the two small aligned perforations tend to fall in the minor ellipse axis.

Genus *PALAEOPONTOSPHAERA* Noël, 1965 emended de Kaenel and Bergen, 1993

**Remarks.** Both de Kaenel and Bergen (1993) and Varol and Girgis (1994) emended *Palaeopontosphaera* to include those Biscutaceae with an inner distal wall. This inner wall displays a bright first-order white birefringence. Two Cretaceous species, which conform to the emended concept of this genus, are transferred to *Palaeopontosphaera* herein.

*Palaeopontosphaera dorsetensis* Varol and Girgis, 1994  
(Pl. 3, Figs. 15, 16)

*Palaeopontosphaera dorsetensis* Varol and Girgis, 1994, p. 243, fig. 8 (A, B), fig. 11 (7, 8).

*Palaeopontosphaera dubia* Noël, 1965  
(Pl. 3, Figs. 12-14)

*Palaeopontosphaera dubia* Noël, 1965 (partim), p. 76-78, pl. 7, figs. 1, 2 (?), 5, 7-10 (non pl. 7, figs. 3, 4, 6, 11-13).  
*Palaeopontosphaera dubia* Noël, 1965; de Kaenel and Bergen, p. 881-882, pl. 1, fig. 15).

*Palaeopontosphaera elliptica* (Górka, 1957) comb. nov.

*Tremalithus ellipticus* Górka, 1957, p. 245, pl. 1, fig. 11.  
*Biscutum ellipticum* (Górka, 1957) Grün and Allemann, 1975, p. 154-156, pl. 1, figs. 5-7, text fig. 3.

**Remarks.** Very small to small forms with a reduced central area and no central spine are identified as *Palaeopontosphaera elliptica*. In cross-polarized light, the tiny central plate exhibits a somewhat bright sigmoidal extinction line separating two darker points. This typical extinction pattern (due to the arrangement of the central granules) and absence of a spine differentiate *Palaeopontosphaera elliptica* from *Palaeopontosphaera dubia*.

*Palaeopontosphaera erismata* Wind and Wise in Wise and Wind, 1977  
(Pl. 3, Figs. 17-19)

*Palaeopontosphaera salebrosa* (Black, 1971) comb. nov.

*Cruciplacolithus salebrosus* Black, 1971, p. 397, pl. 30, fig. 4.  
*Crucibiscuturn salebrosus* (Black, 1971) Jakubowski, 1986, p. 38, pl. 1, figs. 16-17.

**Remarks.** This species is transferred to the genus *Palaeopontosphaera* based on the presence of an inner distal wall. It differs from *Palaeopontosphaera erismata* by its larger size and distinct axial cross structure. *Palaeopontosphaera salebrosa* was observed in Holes 897C, 897C, and 899B.

*Palaeopontosphaera* sp. 1

**Remarks.** In cross-polarized light, this small form of *Palaeopontosphaera* has a bicyclic rim extinction pattern and a faint central plate with two small perforations aligned with the longitudinal axis. The FO of *Palaeopontosphaera* sp. 1 was observed in the upper Aptian in Hole 897C.

*Palaeopontosphaera* sp. 2

**Remarks.** This small circular to subcircular form of *Palaeopontosphaera* has a central cross supporting a solid distal projection, which nearly filled the central area. In cross-polarized light, *Palaeopontosphaera* sp. 2 exhibits a bicyclic rim. The thin inner rim cycle displays a first-order white birefringence, and the broad outer rim cycle is faintly birefringent. The central cross is also brightly birefringent.

*Palaeopontosphaera* sp. 2 differs from *Palaeopontosphaera dorsetensis* by the presence of a central structure.

Genus *PERCIVALIA* Bukry, 1969

*Percivalia arata* sp. nov.  
(Pl. 8, Figs. 3, 12, 14, 15)

**Diagnosis.** A medium-sized species of *Percivalia* with a narrow rim and a central area constructed by numerous, bladed elements arranged in longitudinal rows. A tiny central spine is present.

**Description.** The narrowly elliptical murolith has a narrow rim. The distal shield is low and very narrow; it is constructed of numerous, imbricated elements. The central area is filled with several longitudinal rows of upright, plate-shaped elements. A cycle of elements visible at the outer margin of the central area may represent the proximal shield. A tiny spine projects distally from the center.

The rim exhibits a faint birefringence and the central area is dark when specimens are oriented 45° to the polarizing direction. When parallel to the nicols, the central area becomes faint to weakly birefringent. Distinct longitudinal furrows separate the rim and central area.

Size. 6.0 to 7.0 µm (holotype: 6.7 (am)).

**Differentiation.** *Percivalia arata* is the only known Jurassic species of *Percivalia*. It is distinguished from *Rhagodiscus nebulosus* Bralower, 1989 (in Bralower et al., 1989) and *Percivalia fenestrata* (Worsley, 1971) Wise, 1983 by the orientation and optical properties of its central area elements (i.e., the longitudinal furrows).

**Derivation of name.** From Latin, *arare*: to plow.

**Holotype.** Plate 8, Figure 3.

**Type locality.** ODP Site 901, Iberia Abyssal Plain.

**Type level.** ODP Sample 149-901A-5R-1, 31 cm; early Tithonian

**Occurrence.** Rare in Tithonian sediments from ODP Hole 901 A.

Genus *PICKELHAUBE* Applegate, Covington, and Wise in Covington and Wise, 1987

*Pickelhaube furtiva* (Roth, 1983) Applegate, Covington, and Wise in Covington and Wise, 1987 (Pl. 8, Figs. 18, 19)

Genus *POLYPODORHABDUS* Noël, 1965

*Polypodorhabdus escaigii* Noël, 1965 (Pl. 8, Figs. 10, 11)

Genus *PERISSOCYCLUS* Black, 1971

*Perissocyclus noeliae* Black, 1971 (Pl. 11, Fig. 19)

Genus *RETECAPSA* Black, 1971 emended Grün, 1975

*Retecapsa neocomiana* Black 1971 (Pl. 8, Figs. 16, 17)

*Retecapsa neocomiana* Black, 1971, p. 410, pl. 33, fig. 3.

*Polypodorhabdus beckii* Medd, 1979, p. 66, pl. 6, fig. 6.

**Remarks.** *Retecapsa neocomiana* is reserved for specimens having lateral bars that form eight angular openings of equal size. *Polypodorhabdus beckii* was described for forms with one or two lateral bars in each central quadrant, but its holotype looks nearly identical to that of *Retecapsa neocomiana*. *Cretarhabdus octofenestratus* Bralower, 1989 has circular central openings. *Retecapsa angustiforata* has a much larger central area, circular central openings, and very birefringent axial and lateral bars.

*Retecapsa schizobrachiata* (Gartner, 1968) Grün, 1975

*Vekshinella schizobrachiata* Gartner, 1968, p. 31, pl. 13, figs. 10, 11; pl. 20, fig. 5.

*Cretarhabdus schizobrachiatus* (Gartner, 1968) Bukry, 1969, p. 36, pl. 15, figs. 4-6.

*Retecapsa schizobrachiata* (Gartner, 1968) Grün, in Grün and Allemann, 1975, (non text fig. 17b).

*Cretarhabdus schizobrachiatus* (Gartner, 1968) Bukry, 1969. Bralower, Monechi, and Thierstein, 1989, p. 212, pl. 3, fig. 16.

**Remarks.** The emended concept of *Retecapsa* by Grün (in Grün and Allemann, 1975) included forms with eight or more central openings. *Retecapsa schizobrachiata* is distinguished by an axial cross that trifurcates longitudinally near the inner rim margin. This creates eight central area perforations of unequal size. The length of specimens recovered from Hole 901A range between 5 and 8 µm. *Retecapsa schizobrachiata* is very rare in Tithonian sediments from Hole 901 A. Grün and Zweili (1980) reported this

species from the lower Oxfordian; the holotype was recovered from the Upper Cretaceous.

Genus *RHAGODISCUS* Reinhardt, 1967

*Rhagodiscus achlyostaurion* (Hill, 1976) Doeven, 1983

*Parhabdololithus achlyostaurion* Hill, 1976, p. 145, pl. 9, figs. 24-29.

*Rhagodiscus achlyostaurion* (Hill, 1976) Doeven, 1983, p. 50.

**Remarks.** Early morphotypes of *Rhagodiscus achlyostaurion* are distinguished by their smaller size (less than 5 µm) and relatively small central area. In cross-polarized light, the species is distinguished by (1) a circular spine base that appears as a bright circle with a dark center and (2) a narrow, birefringent inner rim cycle. Bergen (1994) recovered early morphotypes of *R. achlyostaurion* from the upper Barremian of DSDP Hole 534A and the Barremian stratotype. This event is used herein to subdivide the *Micrantholithus hoschulzii* Zone (CC6).

*Rhagodiscus angustus* (Stradner, 1963) Reinhardt, 1971

**Remarks.** Early morphotypes of *Rhagodiscus angustus* are very small and possess narrowly elliptical to subrectangular outlines. More typical forms have parallel longitudinal peripheries, which should be slightly concave. The FO of *R. angustus* (early morphotype) is slightly above that of *Hayesites irregularis* in Holes 897C and 899B, whereas it is 2.2 m below the FO of *H. irregularis* in Hole 897D. This could result from poor core recovery within the Cretaceous or the sporadic occurrence of *H. irregularis* near the bottom of its stratigraphic range.

*Rhagodiscus pseudoangustus* Crux, 1987

*Rhagodiscus pseudoangustus* Crux, 1987, p. 31, pl. 1, figs. 4, 5, 16, 17.

*Zeughrabdotos? pseudoangustus* Bralower, Applegate, Covington, and Wise in Covington and Wise, 1987, p. 633, pl. 8, figs. 2-4.

**Remarks.** *Rhagodiscus pseudoangustus* is identified by its subrectangular outline and large, hollow spine. *Rhagodiscus angustus* has a subrectangular outline with parallel longitudinal peripheries that are slightly concave. It differs from *R. pseudoangustus* by its thick granular plate and the absence of a large, hollow spine. However, the electron micrograph of a specimen in proximal view illustrated by Crux (1987; pl. 1, fig. 5) shows the presence of a central granular plate. A central plate is not visible in the holotype (distal view) designated by Crux (1987; pl. 1, fig. 4), nor are any visible in the original specimens illustrated and described under the same species name by Bralower et al. (in Covington and Wise, 1987). Bralower et al. (in Covington and Wise, 1987) also commented on the absence of a central granular plate in their description of *Zeughrabdotos? pseudoangustus*. Both publications became available in 1987. *Rhagodiscus pseudoangustus* Crux, 1987 was described in April 1987 and has priority over *Zeughrabdotos? pseudoangustus* Bralower et al. (in Covington and Wise; May 1987). The designated holotype of *Rhagodiscus pseudoangustus* Crux, 1987 is better preserved and the presence of a thin, granular plate is assumed to be a preservational artifact.

Genus *ROTELAPILLUS* Noël, 1973

*Rotelapillus pleoseptatus* sp. nov. (Pl. 9, Figs. 14, 19-25)

**Diagnosis.** A small, elliptical species of *Rotelapillus* with a high distal shield and distally extended radial bars.

**Description.** A small elliptical murolith with a high distal shield constructed of vertical elements. The distal rim surface is irregular; its individual elements have pointed extremities of unequal length. The central area is constructed of thick, vertical elements that extend radially from the wall toward the center, but may not be joined at the center (preservational artifact?). In cross-polarized light, the rim is faintly birefringent and the radial central elements exhibit a first-order white birefringence.

Size. 4 to 5 µm (holotype: 4.6 µm).

**Differentiation.** *Rotelapillus pleoseptatus* differs from *Rotelapillus radicans* by its elevated rim and by the higher number of radial bars. It differs from *Rotelapillus laffitei* by its high rim and elliptical shape. *Rotelapillus pleosep-*

*tatus* is differentiated from *Rotelapillus caravacaensis* by its higher number of radial bars.

**Derivation of name.** From Latin, *pleto*: column, and *septum*: partition.

**Holotype.** Plate 9, Figures 14, 22-25; specimen transferred from the LM to the SEM.

**Type locality.** ODP Site 901, Iberia Abyssal Plain.

**Type level.** ODP Sample 149-901A-5R-1, 31 cm; Tithonian

**Occurrence.** Rare to few in Tithonian sediments from ODP Hole 901 A.

*Rotelapillus radians* Noël, 1973  
(Pl. 9, Figs. 3, 15-18)

**Remarks.** *Rotelapillus radians* is an elliptical to subelliptical species with eight radial bars and a low distal shield without any lateral projections. In cross-polarized light, the rim of *Rotelapillus radians* displays a bright, unicyclic birefringence. *Rotelapillus radians* differs from *Rotelapillus caravacaensis* (Grün in Grün and Allemann, 1975) by its narrower and lower distal shield. However, specimens of *R. radians* recovered from Hole 901A have slightly broader distal shields than illustrated by Noël (1973) and are difficult to differentiate from *R. caravacaensis*.

Genus *STEPHANOLITHION* Deflandre, 1939

*Stephanolithion bigotii* Deflandre, 1939 *bigotii* (Medd, 1979)  
(Pl. 9, Figs. 1,4,5)

Genus *STRADNERUTHUS* Black, 1971

*Stradnerlithus asymmetricus* (Rood, Hay, and Barnard, 1971) Noël, 1973  
(Pl. 9, Figs. 2, 6, 7)

*Stradnerlithus sexiramatus* (Pienaar, 1969) Perch-Nielsen, 1984  
(Pl. 9, Figs. 8, 9)

Genus *TETRAPODORHABDUS* Black, 1971

*Tetrapodorhabdus coptensis* Black, 1971  
(Pl. 11, Figs. 12, 13)

Genus *TRANOLITHUS* Stover, 1966

*Tranolithus incus* sp. nov.  
(Pl. 7, Figs. 1,4,7-8)

**Diagnosis.** A small- to medium-sized, elliptical species of *Tranolithus* with four small blocky elements distributed on either side of the longitudinal poles and surrounding a broad, proximal bar (which almost fills the central area). Two small triangular openings are situated on each side of this plate bar.

**Description.** Elliptical murolith with a broad distal shield constructed of imbricated elements. Four blocky, rectangular elements are attached to the inner rim margin and are situated in pairs on either side of longitudinal poles. A thin, rectangular bar spans the central area and is attached to the proximal surface. In cross-polarized light, the rim extinction pattern is unicyclic and faintly birefringent. The four blocky central area elements are slightly more birefringent. The central plate is dark and is visible only in phase contrast illumination.

Size. 4.5 to 6.0  $\mu\text{m}$  (holotype: 5.0  $\mu\text{m}$ )

**Differentiation.** *Tranolithus incus* differs from other *Tranolithus* by its anvil-shaped central opening, proximal bar, and distribution of its four, blocky central elements. *Rhagodiscus pseudoangustus* has a subrectangular outline.

**Derivation of name.** From Latin, *incus*: anvil.

**Holotype.** Plate 7, Figures 1, 4.

**Type locality.** ODP Site 901, Iberia Abyssal Plain.

**Type level.** ODP Sample 149-901A-5R-1, 31 cm; Tithonian

**Occurrence.** Rare in Tithonian sediments from ODP Hole 901 A.

Genus *TRISCUTUM* Dockerill, 1987

*Triscutum* cf. *T. expansum* (Medd, 1979) Dockerill, 1987  
(Pl. 8, Figs. 6-9)

**Remarks.** This medium-sized form of *Triscutum* has a central grill composed of thin diagonal bars separated into four quadrants. It differs from typical specimens of *Triscutum expansum* by its narrow rim and inner wall. In cross-polarized light, the rim extinction pattern exhibits a first-order white bi-

refringence. The four quadrants of the central grill exhibit a faint to white birefringence upon rotation, as opposing quadrants display the same birefringence. *Triscutum* cf. *T. expansum* is very rare to rare in Tithonian sediments from Hole 901 A, but its distinct optical properties enhance its potential biostratigraphic utility.

Genus *THURMANNOLITHION* Grün and Zweili, 1980

*Thurmannolithion clatratum* Grün and Zweili, 1980  
(Pl. 8, Figs. 1,2,4,5)

Genus *TRUNCATOSCAPHUS* Rood, Hay, and Barnard, 1971

*Truncatoscapus senarius* (Wind and Wise in Wise and Wind, 1977)  
Perch-Nielsen, 1984  
(Pl. 9, Figs. 10, 11)

Genus *VAGALAPILLA* Bukry, 1969

*Vagalapilla parallela* (Wind and Cepek, 1979) comb. nov.

*Rhadolekiskus parallelus* Wind and Cepek, 1979, p. 232, pl. 3, figs. 3-6.

"*Rhadolekiskus parallelus*" Wind and Cepek, 1979; Covington and Wise, 1987, p. 632, pl. 23, figs. 3-5.

*Vekshinella parallela* (Wind and Cepek, 1979) Applegate and Bergen, 1988, p. 316, pl. 15, figs. 1-9.

**Remarks.** Applegate and Bergen (1988) demonstrated that the long distal projection of this species is supported by a thin axial cross and placed it within *Vekshinella* Loeblich and Tappan, 1963. *Vagalapilla* Bukry, 1969 is used herein for this group of muroliths because *Vekshinella* is based on a questionable type species and holotype.

Applegate and Bergen (1988) reported *Vagalapilla parallela* in the lower Valanginian of Leg 103 material. Bergen (1994) indicated an early Valanginian appearance for the species in southeastern France and DSDP Hole 534A. The occurrence of *Vagalapilla parallela* in Tithonian section of Hole 901A extends its range into the Jurassic.

*Vagalapilla quadriarculla* (Noël, 1965) Roth, 1983  
(Pl. 10, Figs. 17, 18)

*Vagalapilla stradneri* (Rood, Hay, and Barnard, 1971) Thierstein 1973  
(Pl. 10, Fig. 20)

*Vagalapilla* sp. 1  
(Pl. 10, Figs. 15, 16)

**Remarks.** This small form (4.0 to 4.5  $\mu\text{m}$ ) of *Vagalapilla* has a inner rim cycle and a thin axial cross that exhibit a first-order white birefringence. The outer-rim cycle has a faint birefringence. In *Vagalapilla stradneri* (Pl. 10, Fig. 20), both the rim cycles and the axial cross have a similar faint birefringence. *Vagalapilla quadriarculla* differs from *Vagalapilla* sp. 1 by its arched axial cross bars and by its large circular central perforation.

*Vagalapilla* sp. 1 is rare to few in Tithonian sediments from Hole 901 A.

*Vagalapilla* sp. 2

**Remarks.** This small form of *Vagalapilla* has a bright bicyclic rim extinction pattern with a relatively large inner cycle exhibiting a first-order white birefringence and divided in four by radial extinction lines. The bright axial cross almost fills the central area and exhibits the same birefringence as the inner rim. *Vagalapilla* sp. 2 has its FO in the lower Aptian at Holes 897C, 897D, and 899B.

*Vagalapilla* sp. 3  
(Pl. 10, Figs. 19,21)

**Remarks.** In cross-polarized light, *Vagalapilla* sp. 3 has a bright bicyclic rim extinction and a broad axial cross, which displays a first-order white birefringence. *Vagalapilla* sp. 3 differs from other Jurassic *Vagalapilla* by its bright cross that nearly filled the central area.

Genus *WATZNAUERIA* Reinhardt, 1964

*Watznaueria tubulata* (Grün and Zweili, 1980) comb. nov.  
(Pl. 3, Figs. 9-11)

*Ellipsagelosphaera? tubulata* Grün and Zweili, 1980, p. 258, pl. 3, figs. 5-7, text fig. 16.

**Remarks.** This elliptical to subelliptical form is transferred to *Watznaueria* owing to its open and empty central area. *Watznaueria tubulata* differs from other *Watznaueria* with open central areas in the construction of its distal shield. As illustrated by Grün and Zweili (1980; text fig. 16) and on Plate 3, Figure 9, the elements of the outer distal cycle are vertically elongated and the shield has a tube shape rather than the flat distal shield observed in *Watznaueria ovata*.

Genus *THORACOSPHERA* Kamptner, 1927

*Thoracosphaera* sp. 1  
(Pl. 10, Figs. 3, 8-12)

**Remarks.** This spherical form referred to *Thoracosphaera* is similar in size to calcareous dinofytes from Upper Triassic sediments. *Thoracosphaera* sp. 1 has a small, hollow center and a thick test composed of large rhombic elements. In cross-polarized light, the elements of the test appear radially arranged and pseudo-extinction crosses are observed.

## APPENDIX B

### Calcareous Nannofossils Considered in This Paper, Listed by Generic Epithet

Tithonian taxa are from Site 901, and Cretaceous taxa are from Sites 897 and 899. The entries not found in the references for the following taxa are given by Perch-Nielsen (1985).

- Anfractus harrisonii* Medd, 1979  
*Ansulasphaera covingtonii* sp. nov.  
*Assipetra infracretacea* (Thierstein, 1971) Roth, 1973  
*Assipetra terebrodentarius* (Applegate, Bralower, Covington, and Wise in Covington and Wise, 1987) Rutledge and Bergen in Bergen, 1994  
*Axopodorhabdus cylindratus* (Noël, 1965) Wind and Wise in Wise and Wind, 1977  
*Axopodorhabdus depravatus* Grün and Zweili, 1980  
*Axopodorhabdus dietzmannii* (Reinhardt, 1965) Wind and Wise in Wise and Wind, 1977  
*Axopodorhabdus rahla* (Noël, 1965) Grün and Zweili, 1980  
*Axopodorhabdus* sp., small  
*Biscutum rotatorium* (Bukry, 1969) comb. nov.  
*Braarudosphaera bigelowii* (Gran and Braarud, 1935) Deflandre, 1947  
*Braarudosphaera regularis* Black, 1973  
*Bukryolithus ambiguus* Black, 1971  
*Calcicalathina oblongata* (Worsley, 1971) Thierstein, 1971  
*Calcicalathina* sp. A of Bergen, 1994  
*Calcivascularis* sp. 1  
*Calyculus* sp., large  
*Chiastozygus leptostaurus* Cooper, 1987  
*Chiastozygus litterarius* (Gorka, 1957) Manivit, 1971  
*Chiastozygus tenuis* Black, 1971  
*Clepsilithus meniscus* sp. nov.  
*Conusphaera mexicana* Trejo, 1969 ssp. *mexicana* (Bralower, 1989)  
*Conusphaera mexicana* Trejo, 1969 ssp. *minor* Bralower ex Bown and Cooper, 1989a  
*Conusphaera rothii* (Thierstein, 1971) Jakubowski, 1986  
*Conusphaera sinespina* sp. nov.  
*Corollithion achylosum* (Stover, 1966) Thierstein, 1971  
*Corollithion acutum* Thierstein, 1972 in Roth and Thierstein, 1972  
*Corollithion protosignum* Worsley, 1971  
*Crepidolithus parvulus* sp. nov.  
*Cretarhabdus conicus* Bramlette and Martini, 1964  
*Cretarhabdus surirellus* (Deflandre in Deflandre and Fert, 1954) Thierstein, 1971  
*Crucellipsis cuvillieri* (Manivit, 1966) Thierstein, 1971  
*Cyclagelosphaera deflandrei* Manivit, 1966  
*Cyclagelosphaera deflandrei* Manivit, 1966 morphotype A  
*Cyclagelosphaera deflandrei* Manivit, 1966 morphotype B  
*Cyclagelosphaera lacuna* Varol and Girgis, 1994  
*Cyclagelosphaera margerelii* Noël, 1965  
*Cyclagelosphaera wiedmannii* Riele and Monechi, 1994  
*Diadorhombus rectus* Worsley, 1971  
*Diadorhombus scutulatus* (Medd, 1971) Medd, 1979  
*Diazomatolithus galicianus* sp. nov.  
*Diazomatolithus lehmanii* Noël, 1965  
*Diloma galiciense* Bergen, 1994  
*Discorhabdus patulus* (Deflandre and Fert, 1954) Noël, 1965  
*Discorhabdus tubus* Noël, 1965  
*Duplexipodorhabdus plethotretus* (Wind and Cepek, 1979 ex Applegate, Covington, and Wise in Covington and Wise, 1987) Varol and Girgis, 1994  
*Eiffellithus primus* Applegate and Bergen, 1988  
*Eiffellithus* sp. small  
*Ellipsagelosphaera britannica* (Stradner, 1963) Perch-Nielsen, 1968  
*Ellipsagelosphaera communis* (Reinhardt, 1964) Perch-Nielsen, 1968  
*Ellipsagelosphaera reinhardtii* (Rood, Hay, and Barnard, 1971) Noël, 1973  
*Ellipsagelosphaera* spp. (small)  
*Ellipsagelosphaera* spp. (large; >13 µm)  
*Eprolithus floralis* (Stradner, 1963) Stover, 1966  
*Ethmorhabdus anglicus* Rood, Hay, and Barnard, 1971  
*Ethmorhabdus gallicus* Noël, 1965  
*Ethmorhabdus hauterivianus* (Black, 1971) Applegate, Covington, and Wise in Covington and Wise, 1987  
*Ethmorhabdus rimosus* Grün and Zweili, 1980  
*Ethmorhabdus* sp. 1  
*Faviconus multicolonnatus* Bralower in Bralower, Monechi, and Thierstein, 1989  
*Flabellites oblongus* (Bukry, 1969) Crux, 1982  
*Grantarhabdus bukryi* Black, 1972  
*Grantarhabdus bukryi* (offset bar)  
*Grantarhabdus meddii* Black, 1971  
*Hayesites irregularis* (Thierstein, 1971) Applegate, Covington, and Wise in Covington and Wise, 1987  
*Hexalithus noelae* Noël, 1957 ex Loeblich and Tappan, 1966  
*Hexapodorhabdus cuvillieri* Noël, 1965  
*Lithraphidites bollii* (Thierstein, 1971) Thierstein, 1973  
*Lithraphidites carniolensis* Deflandre, 1963  
*Lotharingius sigillatus* (Stradner, 1961) Prins in Grün, Prins, and Zweili, 1974  
*Lucianorhabdus salomonii* Bergen, 1994  
*Manivitella pemmatoidea* (Deflandre ex Manivit, 1965) Thierstein, 1971  
*Markalius circumradiatus* (Stover, 1966) Roth, 1978  
*Markalius ellipticus* Grün in Grün and Allemann 1975  
*Micrantholithus hoschulzii* (Reinhardt, 1966) Thierstein, 1971  
*Micrantholithus obtusus* Stradner, 1963  
*Microstaurus chiastus* (Worsley, 1971) Grün in Grün and Allemann, 1975  
*Microstaurus conus* Wind and Cepek, 1979  
*Microstaurus quadratus* Black, 1971  
*Miravetesina favula* Grün in Grün and Allemann, 1975  
*Nannoconus abundans* Stradner, 1963  
*Nannoconus bermudezi* Brönnimann, 1955  
*Nannoconus bucheri* Brönnimann, 1955  
*Nannoconus globulus* Brönnimann, 1955  
*Nannoconus kamptneri kamptneri* Brönnimann, 1955  
*Nannoconus ligius* Applegate and Bergen, 1988  
*Nannoconus steinmannii steinmannii* Kamptner, 1931  
*Nannoconus truitti* Brönnimann, 1955  
*Nodosella* cf. *N. silvaradion*  
*Octopodorhabdus decussatus* (Manivit, 1961) Rood, Hay, and Barnard, 1971  
*Octopodorhabdus oculisminutis* Grün and Zweili, 1980  
*Octopodorhabdus praevisus* Noël, 1965  
*Palaeopontosphaera dorsetensis* Varol and Girgis, 1994  
*Palaeopontosphaera dubia* Noël, 1965  
*Palaeopontosphaera elliptica* (Gorka, 1957) comb. nov.  
*Palaeopontosphaera erismata* Wind and Wise in Wise and Wind, 1977  
*Palaeopontosphaera salebrosa* (Black, 1971) comb. nov.  
*Palaeopontosphaera* sp. 1  
*Palaeopontosphaera* sp. 2  
*Percivalia arata* sp. nov.  
*Percivalia fenestrata* (Worsley, 1971) Wise, 1983  
*Perissocyclus fletcheri* Black, 1971  
*Perissocyclus noeliae* Black, 1971  
*Perissocyclus tayloriae* Crux, 1989

- Pickelhaube furtiva* (Roth, 1983) Applegate, Covington, and Wise in Covington and Wise, 1987  
*Polypodorhabdus escaigii* Noël, 1965  
*Polypodorhabdus madingleyensis* Black, 1971  
*Prediscosphaera spinosa* (Bramlette and Martini, 1964) Gartner, 1968  
*Proculithus charlottei* Medd 1979  
*Pseudocomus enigma* Bown and Cooper, 1989a  
*Reinhardtites scutula* Bergen, 1994  
*Retecapsa angustiforata* Black, 1971  
*Retecapsa neocomiana* Black, 1971  
*Retecapsa radiata* (Worsley, 1971) Applegate and Bergen, 1988  
*Retecapsa schizobrachiata* (Gartner, 1968) Grün in Grün and Allemann, 1975  
*Rhagodiscus achlyostaurion* (Hill, 1976) Doeven, 1983  
*Rhagodiscus angustus* (Stradner, 1963) Reinhardt, 1971  
*Rhagodiscus asper* (Stradner, 1963) Reinhardt, 1967  
*Rhagodiscus infinitus* (Worsley, 1971) Applegate, Covington, and Wise in Covington and Wise, 1987  
*Rhagodiscus pseudoangustus* Crux, 1987  
*Rhagodiscus splendens* (Deflandre, 1953) Verbeek, 1977  
*Rhombolithion rhombicum* (Stradner and Adamiker, 1966) Black, 1973  
*Rotelapillus laffitei* (Noël, 1957) Noël, 1973  
*Rotelapillus pleoseptatus* sp. nov.  
*Rotelapillus radians* Noël, 1973  
*Sollasites concentricus* Rood, Hay, and Barnard, 1971  
*Sollasites horticus* (Stradner, Adamiker, and Maresch in Stradner and Adamiker, 1966) Cepek and Hay, 1969  
*Speetonia colligata* Black, 1971  
*Staurolithites mutterlosei* Crux, 1989  
*Stephanolithion ametros* Cooper, 1987  
*Stephanolithion bigotii* Deflandre, 1939 ssp. *bigotii* 1979  
*Stradnerlithus asymmetricus* (Rood, Hay, and Barnard, 1971) Noël, 1973  
*Stradnerlithus comptus* Black, 1971  
*Stradnerlithus sexiramatus* (Pienaar, 1969) Perch-Nielsen, 1984  
*Tegumentum stradneri* Thierstein in Roth and Thierstein, 1972  
*Tetrapodorhabdus coptensis* Black, 1971  
*Thoracosphaera* sp. 1  
*Thurmannolithion clatratum* Grün and Zweili, 1980  
*Tranolithus incus* sp. nov.  
*Triscutum* cf. *T. expansum*  
*Truncatoscapus senarius* (Wind and Wise in Wise and Wind, 1977) Perch-Nielsen, 1984  
*Tubirhabdus patulus* Prins, 1969 ex Rood, Hay, and Barnard, 1973  
*Tubodiscus jurapelagicus* (Worsley, 1971) Roth, 1973  
*Tubodiscus veranae* Thierstein, 1973  
*Umbria granulosa* ssp. *minor* Bralower and Thierstein in Bralower, Monechi, and Thierstein, 1989  
*Vagalapilla parallela* (Wind and Cepek, 1979) comb. nov.  
*Vagalapilla quadriarcula* (Noël, 1965) Roth, 1983  
*Vagalapilla* sp. 1  
*Vagalapilla* sp. 2  
*Vagalapilla* sp. 3  
*Vagalapilla stradneri* (Rood, Hay, and Barnard, 1971) Thierstein, 1973  
*Watznaueria barnesae* (Black in Black and Barnes, 1959) Perch-Nielsen, 1968  
*Watznaueria biporta* Bukry, 1969  
*Watznaueria fossacincta* (Black, 1971) Bown in Bown and Cooper, 1989b  
*Watznaueria manivittae* Bukry, 1973  
*Watznaueria ovata* Bukry, 1969  
*Watznaueria tubulata* (Grün and Zweili, 1980) comb. nov.  
*Zeugrhabdotus hoffatii* Rood, Hay, and Barnard, 1973  
*Zeugrhabdotus embergeri* (Noël, 1959) Perch-Nielsen, 1984  
*Zeugrhabdotus erectus* (Deflandre in Deflandre and Fert, 1954) Reinhardt, 1965  
*Zeugrhabdotus erectus* (thick bar)  
*Zeugrhabdotus fissus* Grün and Zweili, 1980  
*Zeugrhabdotus noeliae* Rood, Hay, and Barnard, 1971  
*Zeugrhabdotus trivectis* Bergen, 1994  
*Zygodiscus diplogrammus* (Deflandre in Deflandre and Fert, 1954) Gartner, 1968  
*Zygodiscus elegans* Gartner, 1968  
*Zygodiscus xenotus* (Stover, 1966) Risatti, 1973

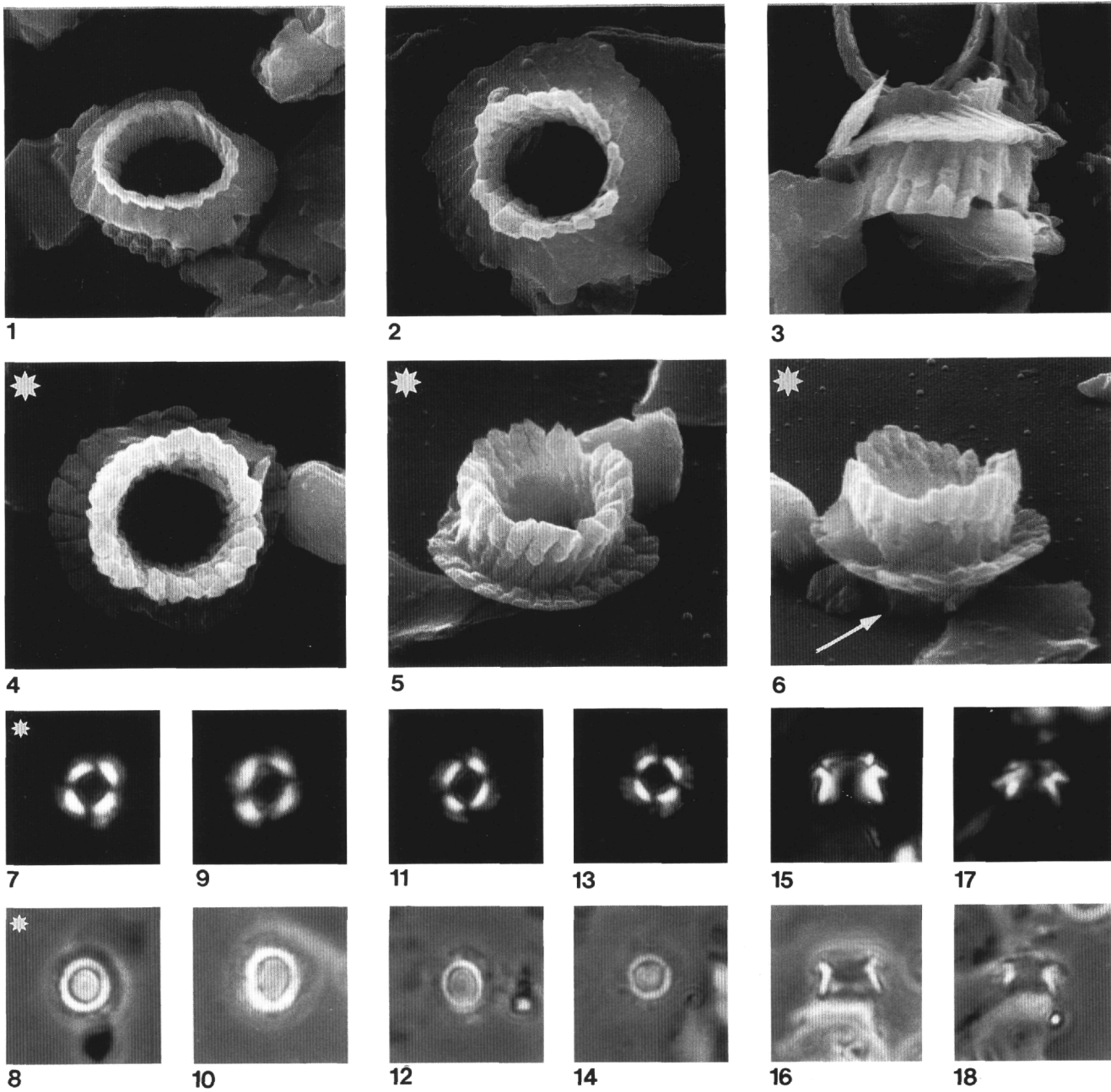


Plate 1. The illustrations of the Plates 1-10 are scanning electron (SEM) and light microscope (LM) micrographs. XP = cross-polarized light; Ph = phase contrast. Transferred specimens from the LM to the SEM are denoted on the plate captions by the superscript<sup>TR</sup>. Magnification for all LM micrographs is X2500 and magnification for SEM micrographs as indicated ( $\times 6000$ ,  $\times 8000$ , or  $\times 12,000$ ). Holotype specimens are indicated by an asterisk. *Ansalasphaera covingtonii* sp. nov.; all SEM specimens from Sample 149-901A-5R-1, 31 cm. **1.** Oblique distal view, FSU-F4. **2.** Distal view, FSU-F118. **3.** Lateral view, FSU-F3. **4-8<sup>TR</sup>**. Holotype, same specimen. **(4)** Proximal view, FSU-F68. **(5)** Oblique proximal view, FSU-F69. **(6)** Oblique proximal view, turned 180° as compared to Figure 5, FSU-F70. **(7)** XP, FSU-FO51-D26. **(8)** Ph, FSU-FO51-D25. **9, 10.** 149-901A-3R-1, 2 cm; XP, FSU-FO41-D35 and Ph, FSU-FO41-D36. **11, 12.** 149-901A-5R-1, 31 cm; XP, FSU-FO44-D4 and Ph, FSU-FO44-D5. **13, 14.** 149-901A-5R-1, 31 cm; XP, FSU-FO45-D3 and Ph, FSU-FO45-D4. **15, 16.** 149-901A-5R-1, 31 cm; XP, FSU-FO46-D13 and Ph, FSU-FO46-D14. **17, 18.** 149-901A-5R-1, 31 cm; XP, FSU-FO45-D18 and Ph, FSU-FO45-D19. Magnification for all SEM micrographs is  $\times 8000$ .

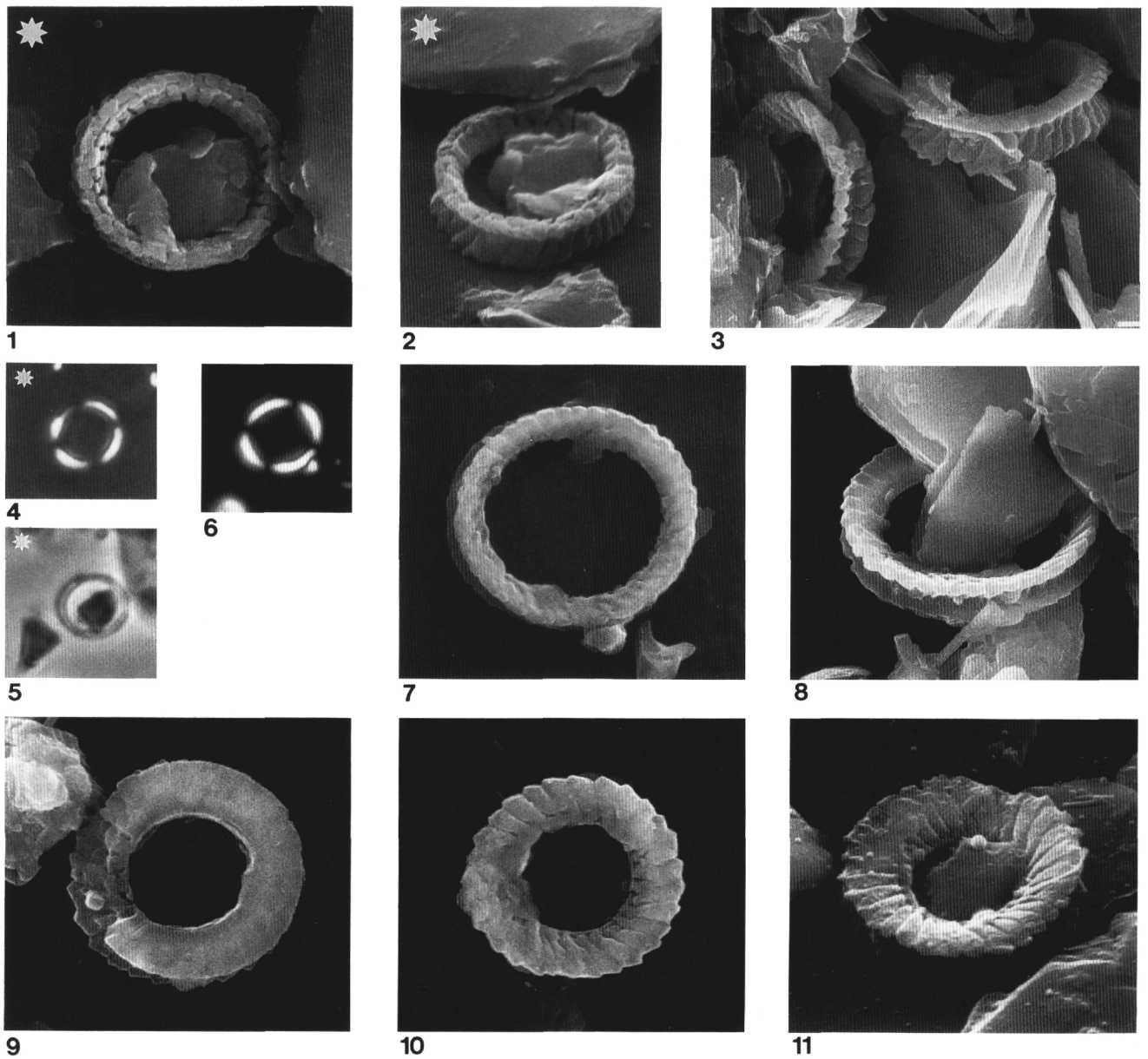


Plate 2. **1-8.** *Diazomatolithus galicianus* sp. nov.; Sample 149-901A-5R-1, 31 cm. (1, 2, 4, 5)<sup>TR</sup>. Holotype, same specimen. (1) Distal view, FSU-F60. (2) Oblique distal view, FSU-F59. (4) XP, FSU-FO51-D17. (5) Ph, FSU-FO51-D18. (3) Oblique proximal view (to the left) and oblique distal view (to the right), FSU-F49. (6, 7)<sup>TR</sup> Isotype, same specimen. (6) XP, FSU-FO52-D26. (7) Proximal view, FSU-F98. (8) Oblique proximal view, FSU-F25. **9-11.** *Diazomatolithus lehmanii* Noël, Sample 149-901A-5R-1, 31 cm. (9) Distal view, FSU-F7. (10) Proximal view, FSU-F38. (11) Oblique proximal view, FSU-F57. Magnification for all SEM micrographs is  $\times 8000$ .

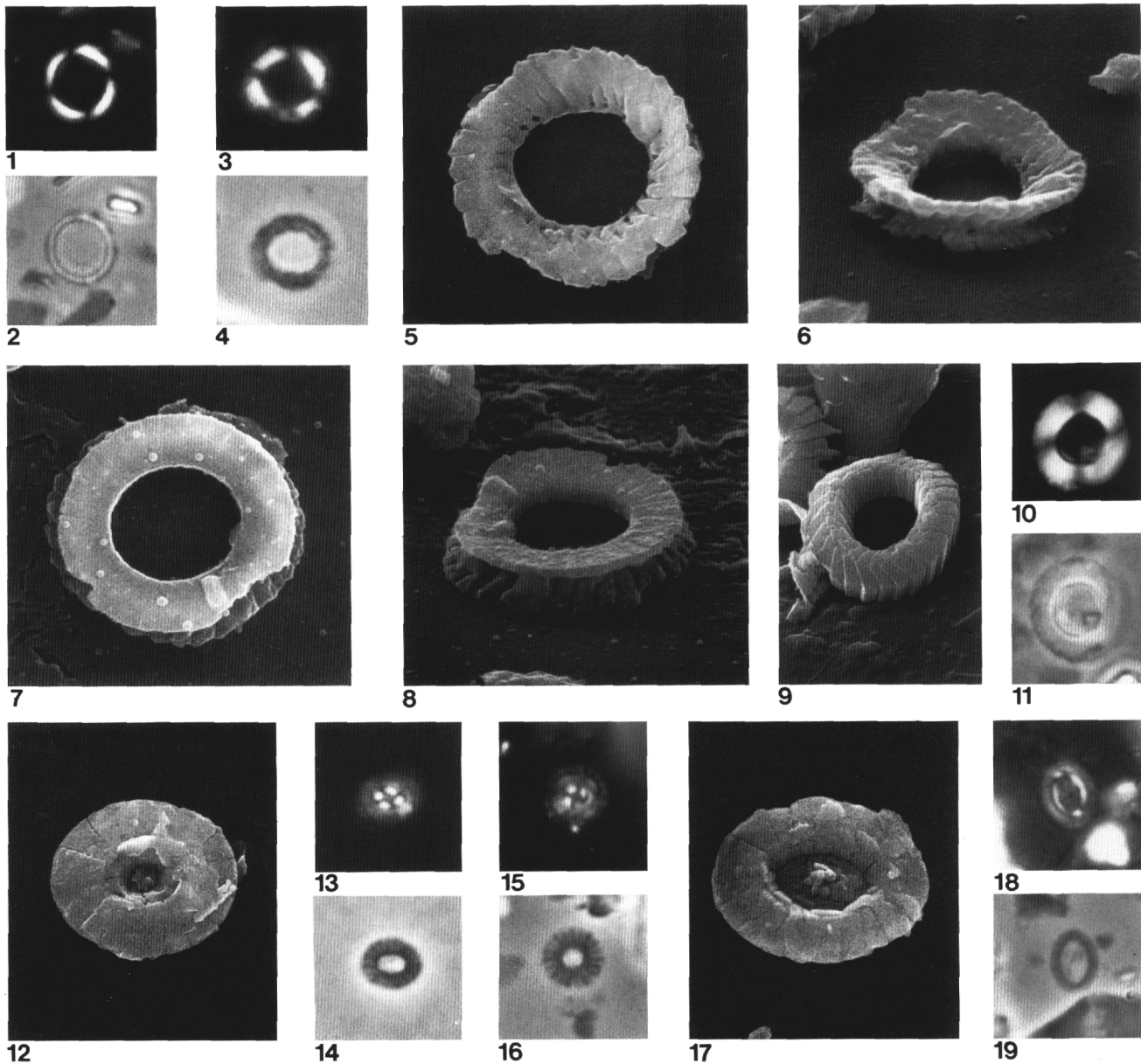


Plate 3. **1, 2.** *Diazomatolithus galicianus* sp. nov.; Sample 149-901A-5R-1, 31 cm; XP, FSU-FO45-D29 and Ph, FSU-FO45-D30. **3-6**<sup>TR</sup>. *Diazomatolithus lehmanii* Noël, same specimen, Sample 149-901A-5R-1, 31 cm. (3, 4) XP, FSU-FO52-D15 and Ph, FSU-FO52-D16. (5) Proximal view, FSU-F107,  $\times 8000$ . (6) Oblique proximal view, FSU-F93,  $\times 8000$ . **7, 8.** *Diazomatolithus lehmanii* Noël, same specimen, Sample 149-901A-5R-1, 31 cm. (7) Distal view, FSU-F82,  $\times 8000$ . (8) Oblique distal view, FSU-F71,  $\times 8000$ . **9-11.** *Watznaueria tubulata* (Grün and Zweili, 1980) comb. nov. (9) Oblique distal view, Sample 149-901A-5R-1, 31 cm; FSU-F48,  $\times 8000$ . (10, 11) Sample 149-901A-5R-1, 31 cm; XP, FSU-FO47-D19 and Ph, FSU-FO47-D20. **12-14**<sup>TR</sup>. *Palaeopontosphaera dubia* Noël, same specimen, Sample 149-901A-5R-1, 31 cm. (12) Distal view, FSU-F108,  $\times 8000$ . (13, 14) XP, FSU-FO52-D17 and Ph, FSU-FO52-D19. **15, 16.** *Palaeopontosphaera dorsetensis* Varol and Girgis, Sample 149-901A-3R-1, 2 cm; XP, FSU-FO41-D31 and Ph, FSU-FO41-D32. **17-19.** *Palaeopontosphaera erismata* Wind and Wise. (17) Distal view, FSU-F11, Sample 149-901A-5R-1, 31 cm;  $\times 12,000$  (2.75  $\mu\text{m}$ ). (18, 19) XP, Sample 149-901A-5R-1, 74 cm; FSU-FO39-D35 and Ph, FSU-F039-D36.

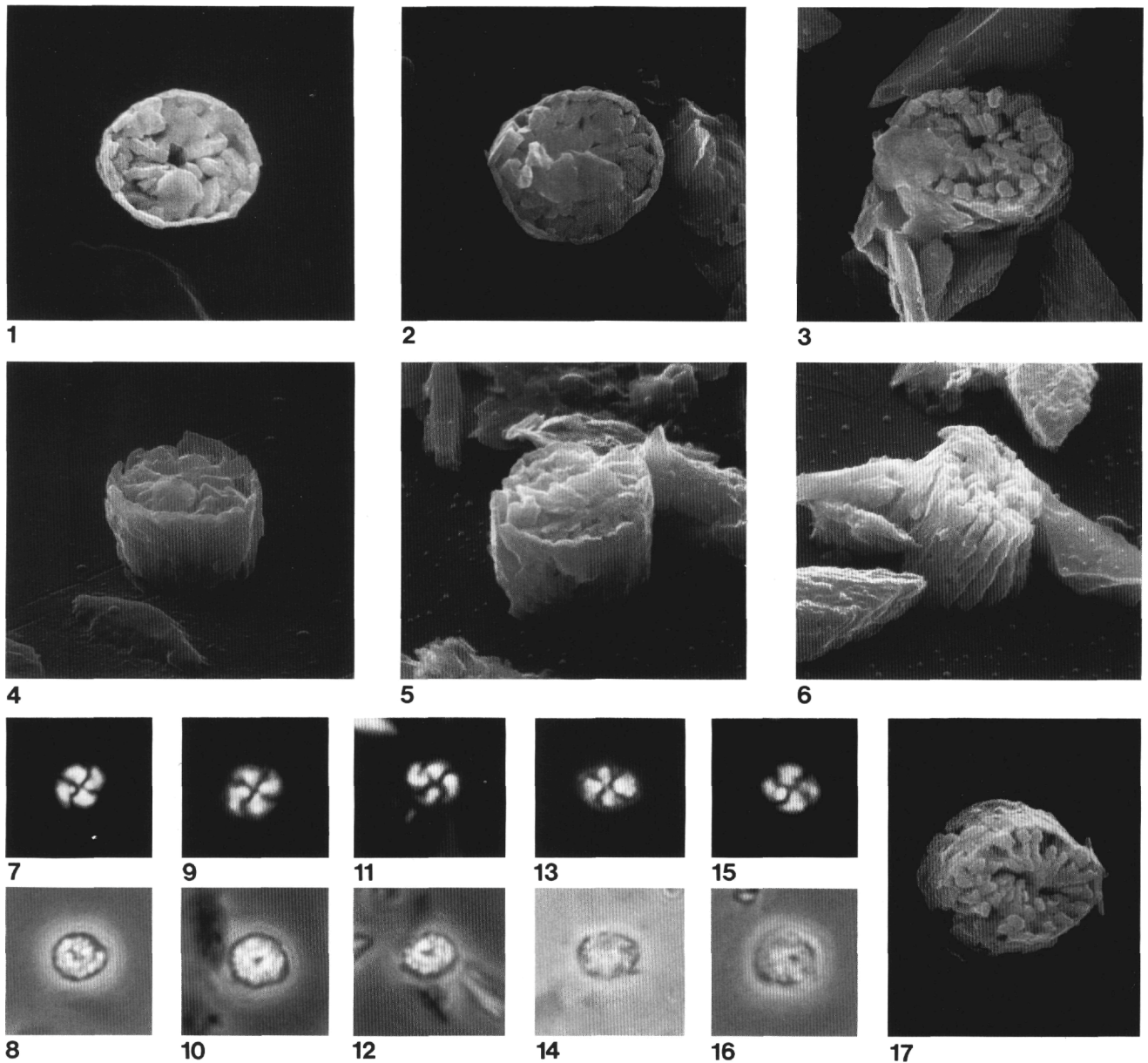


Plate 4. **1-12, 15-17.** *Conusphaera mexicana* Trejo ssp. *minor* Bralower ex Bown and Cooper, Sample 149-901A-5R-1, 31 cm. (1, 4, 7, 8)<sup>TR</sup>. Same specimen. (1) Distal view, FSU-F103. (4) Oblique distal view, FSU-F115. (7, 8) XP, FSU-FO52-D9 and Ph, FSU-FO52-D10. (2, 5, 9, 10)<sup>TR</sup>. Same specimen (2) Distal view, FSU-F66. (5) Oblique distal view, FSU-F78. (9, 10) XP, FSU-FO51-D21 and Ph, FSU-FO51-D23. (3, 6, 11, 12)<sup>TR</sup>. Same specimen (3) Proximal view, FSU-F62. (6) Oblique proximal view, FSU-F115. (11, 12) XP, FSU-FO51-D19 and Ph, FSU-FO51-D20. (15, 16, 17)<sup>TR</sup>. Same specimen. (15, 16) XP, FSU-FO52-D1 and Ph, FSU-FO52-D2. (17) Proximal view, FSU-F100. **13, 14.** *Conusphaera* cf. *C. mexicana* ssp. *minor*. Elliptical specimen, Sample 149-901A-3R-1, 1 cm; XP, FSU-FO41-D3 and Ph, FSU-FO41-D4. Magnification for all SEM micrographs is  $\times 8000$ .

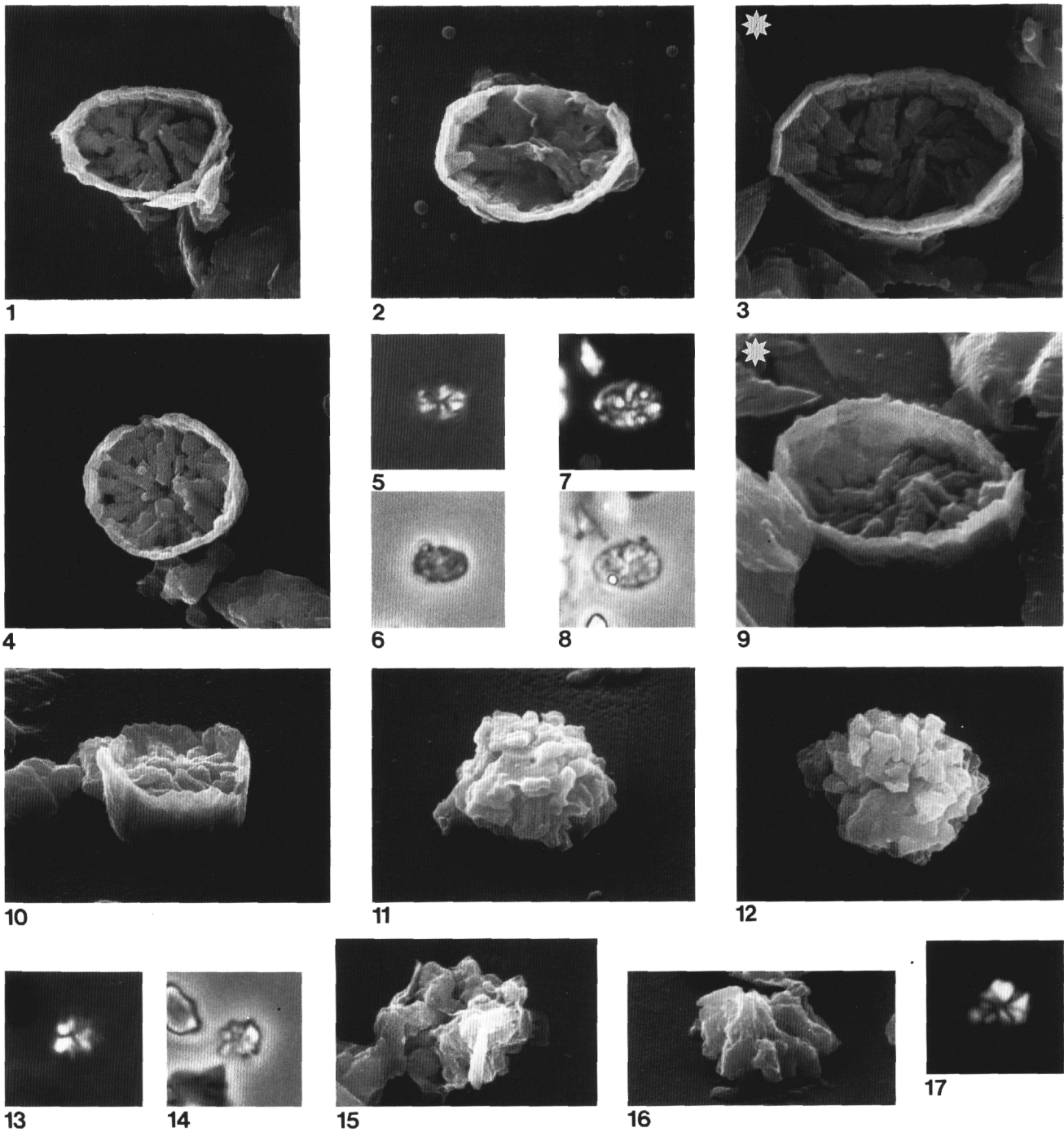


Plate 5. **1-3, 5-9.** *Conusphaera sinespina* sp. nov. (1) Distal view, Sample 149-901A-5R-1, 31 cm; FSU-F111,  $\times 8000$ . (2, 5, 6 )<sup>TR</sup>. Same specimen, Sample 149-901A-5R-1, 31 cm. (2) Distal view, FSU-F54,  $\times 10000$ . (5, 6) XP, FSU-FO51-D11 and Ph, FSU-FO51-D14. (3, 9) Holotype, same specimen, Sample 149-301A-5R-1, 31 cm. (3) Distal view, FSU-F74,  $\times 12,000$ . (9) Oblique distal view, FSU-F77,  $\times 12,000$ . (7, 8) Sample 149-901A-3R-1, 2 cm; XP, FSU-FO41-D6 ind Ph, FSU-FO41-D7. **4, 10.** *Conusphaera mexicana* Trejo ssp. *minor* Bralower ex Cooper, same specimen, Sample 149-901A-5R-1, 31 cm. (4) Distal view, FSU-F12,  $\times 8000$ . (10) Oblique distal view, FSU-F13,  $\times 8000$ . **11-17.** Broken spine of *Conusphaera mexicana* Trejo ssp. *minor* Bralower ex Bown and Cooper, Sample 149-901A-5R-1, 31 cm. (11, 12, 17)<sup>TR</sup>. Same specimen. (11) Oblique proximal view, FSU-F92,  $\times 8000$ . (12) Proximal view, FSU-F89,  $\times 8000$ . (17) XP, FSU-F052-D44. (13-16)<sup>TR</sup>. Same specimen. (13, 14) XP, FSU-FO52-D41 and Ph, FSU-FO52-D42. (15) Proximal view, FSU-F90,  $\times 8000$ . (16) Oblique proximal view, FSU-F84,  $\times 8000$ .

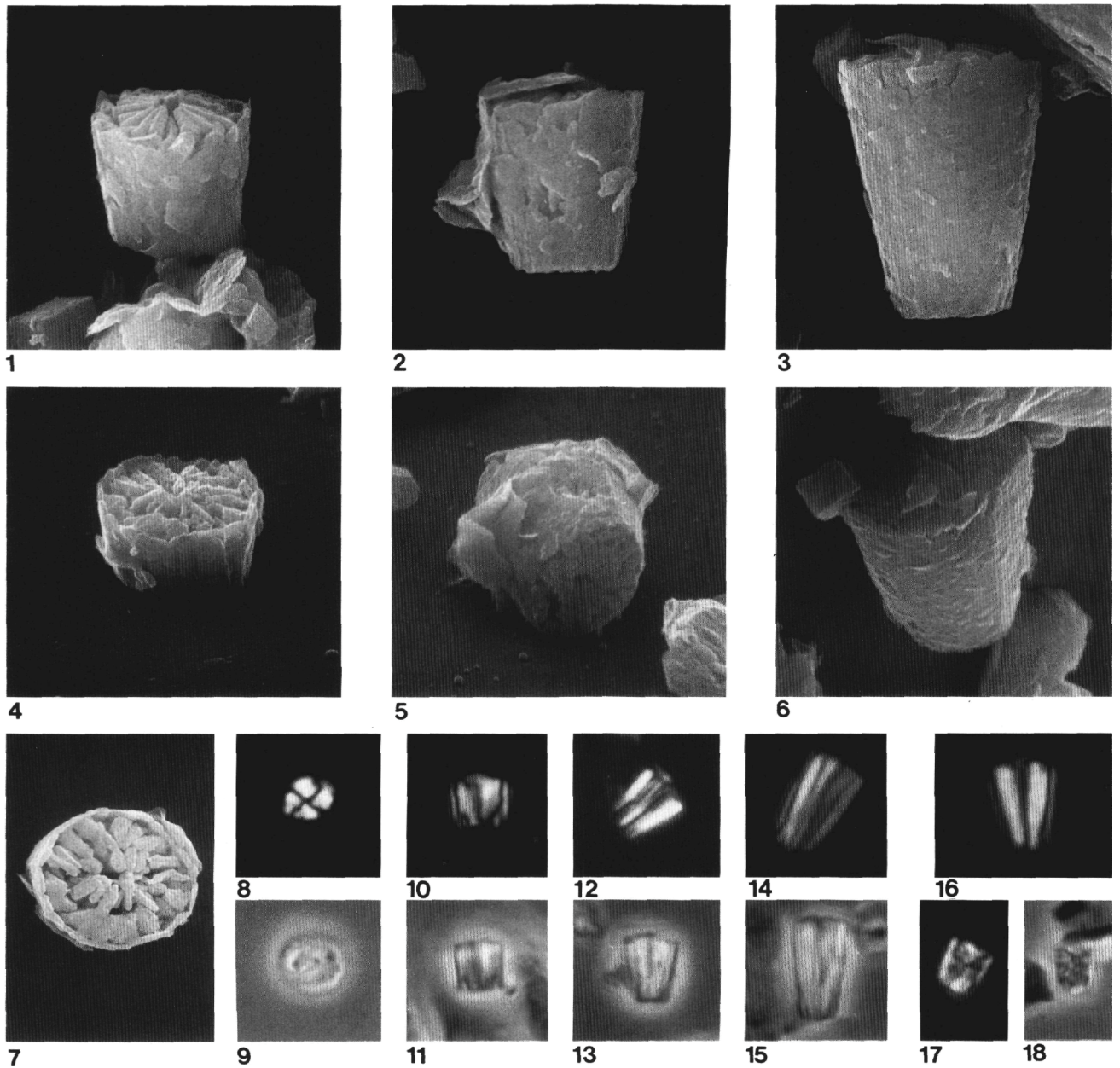


Plate 6. **1, 2, 4, 5, 7-13.** *Conusphaera mexicana* Trejo ssp. *minor* Bralower ex Bown and Cooper, Sample 149-901A-5R-1, 31 cm. (1) Oblique distal view, FSU-F85. (2, 5, 12, 13)<sup>TR</sup>. Same specimen. (2) Lateral view, FSU-F63. (5) Oblique proximal view, FSU-F76. (12, 13) XP, FSU-FO51-D12 and Ph, FSU-FO51-D15. (4, 7-9)<sup>TR</sup>. Same specimen. (4) Oblique distal view, FSU-F116. (7) Distal view, FSU-F104. (8, 9) XP, FSU-FO52-D7 and Ph, FSU-FO52-D8. (10-11) XP, FSU-FO44-D31 and Ph, FSU-F044-D32. **3, 6, 14-16.** *Conusphaera mexicana* Trejo ssp. *mexicana* (1989). (3, 6, 16)<sup>TR</sup>. Same specimen, Sample 149-901A-5R-1, 31 cm. (3) Lateral view, FSU-F88. (6) Oblique distal view, FSU-F91. (16) XP (at 90°), FSU-FO52-D43. (14, 15) XP (at 45°), Sample 149-901A-6R-1, 131 cm; FSU-FO39-D8 and Ph, FSU-FO39-D9. **17, 18.** *Calxivascularis* sp. 1, Sample 149-901A-5R-1, 31 cm; XP (at 90°), FSU-FO44-D6 and Ph, FSU-FO44-D7. Magnification for all SEM micrographs is  $\times 8000$ .

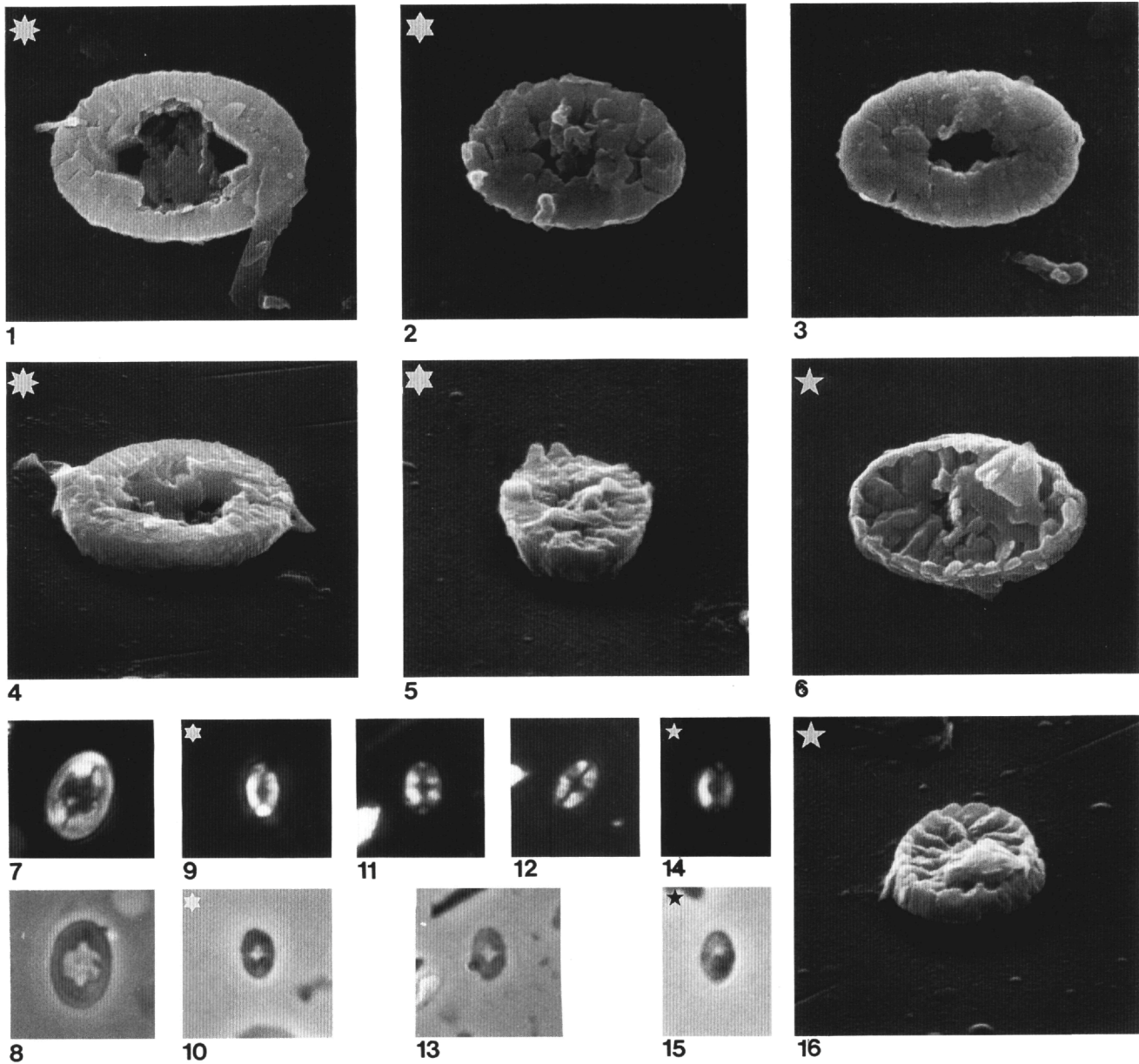


Plate 7. **1, 4, 7, 8.** *Tranolithus incus* sp. nov. (1,4) Holotype, same specimen, Sample 149-901A-5R-1, 31 cm. (1) Distal view, FSU-F113,  $\times 8000$ . (4) Oblique distal view, FSU-F114,  $\times 8000$ . (7, 8) XP, Sample 149-901A-3R-1, 33 cm; FSU-FO47-D36 and Ph, FSU-FO47-D37. **2, 3, 5, 9-13.** *Crepidolithus parvulus* sp. nov.; Sample 149-901A-5R-1, 31 cm. (2, 5, 9, 10)<sup>TR</sup>. Holotype, same specimen, Sample 149-901A-5R-1, 31 cm. (2) Distal view, FSU-F101,  $\times 12,000$ . (5) Oblique distal view, FSU-F95,  $\times 12,000$ . (9, 10) XP, FSU-FO52-D3 and Ph, FSU-FO52-D4. (3) Distal view, FSU-F86,  $\times 12,000$ . (11-13) XP (at  $90^\circ$ ), FSU-FO41-D12; XP (at  $45^\circ$ ), FSU-FO41-D11 and Ph, FSU-FO41-D10, Sample 149-901A-3R-1, 2 cm. **6, 14-16**<sup>TR</sup>. *Clepsilithus meniscus* sp. nov.; holotype, same specimen, Sample 149-901A-5R-1, 31 cm. (6) Proximal view, FSU-F102,  $\times 12,000$ . (16) Oblique proximal view, FSU-F95,  $\times 12,000$ . (14, 15) XP, FSU-FO52-D4 and Ph, FSU-FO52-D6.

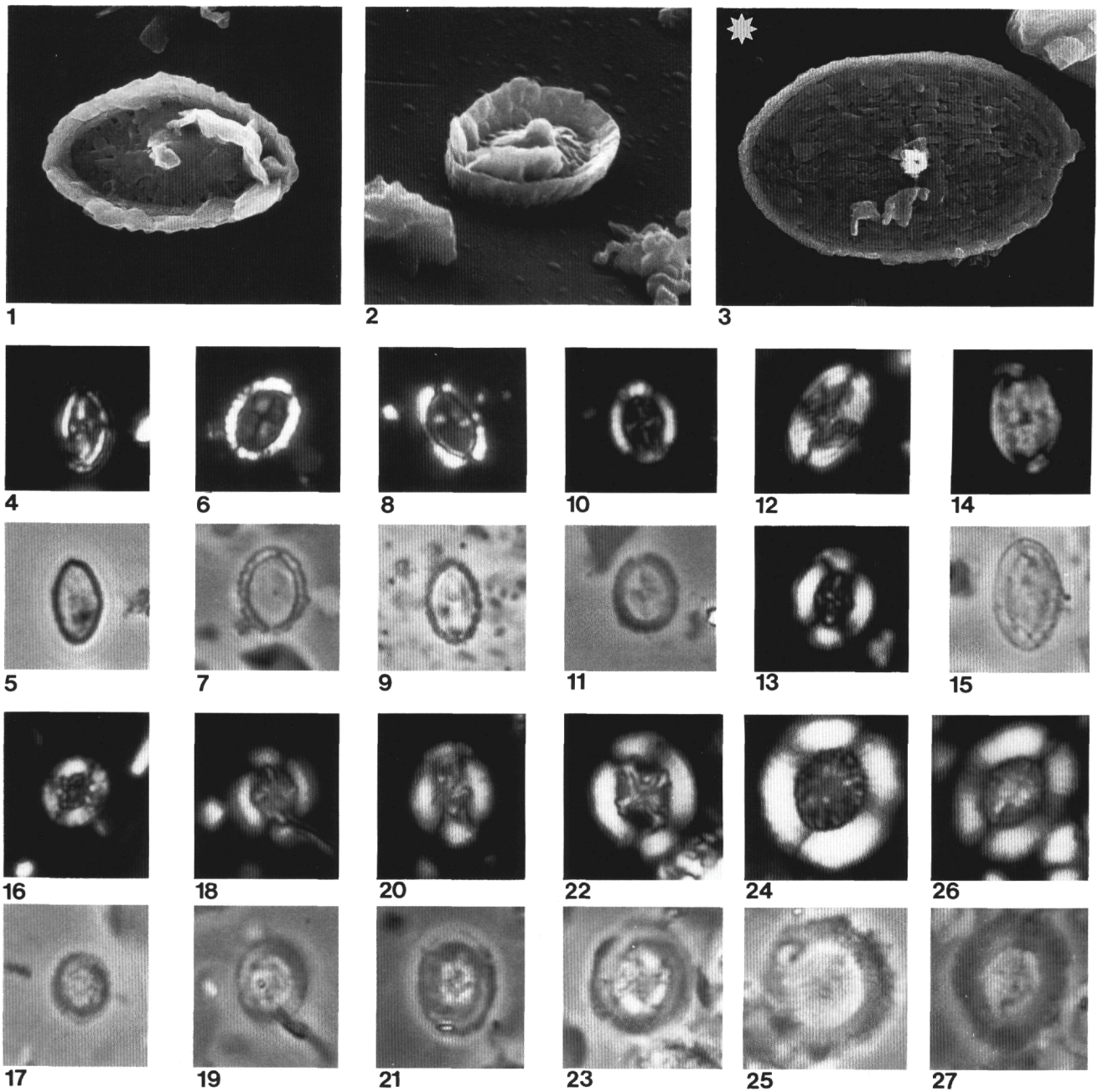


Plate 8. **1, 2, 4, 5<sup>TR</sup>**. *Thurmannelithion clatratum* Grün and Zweili, same specimen, Sample 149-901A-5R-1, 31 cm. (1) Distal view, FSU-F105,  $\times 8000$ . (2) Oblique distal view, FSU-F106,  $\times 8000$ . (**4, 5**) XP, FSU-FO52-D11 and Ph, FSU-FO52-D12. **3, 12, 14, 15**. *Percivalia arata* sp. nov., Sample 149-901A-5R-1, 31 cm. (3) Holotype, distal view, FSU-F35,  $\times 8000$ . (**12, 14, 15**) XP (at  $45^\circ$ ), FSU-FO49-D22, XP (at  $90^\circ$ ), FSU-FO49-D23 and Ph, FSU-FO49-D24. **6-9**. *Triscutum* cf. *T. expansum*. (**6, 7**) XP, Sample 149-901A-6R-1, 131 cm; FSU-FO39-D5 and Ph, FSU-FO39-D6. (**8, 9**) XP, Sample 149-901A-5R-1, 31 cm; FSU-FO52-D25 and Ph, FSU-FO52-D29. **10, 11**. *Polypodorhabdus escaigii* Noël; XP, Sample 149-901A-3R-1, 2 cm; FSU-FO41-D28 and Ph, FSU-FO41-D29. **13**. *Polypodorhabdus madingleyensis* Black; XP, Sample 149-901A-3R-1, 2 cm; FSU-FO52-D42. **16, 17**. *Retecapsa neocomiana* Black; XP, Sample 149-901A-5R-1, 31 cm; FSU-FO46-D9 and Ph, FSU-FO46-D10. **18, 19**. *Pickelhaube furtiva* (Roth) Applegate, Covington and Wise; XP, Sample 149-901A-5R-1, 31 cm; FSU-FO46-D26 and Ph, FSU-FO46-D27. **20, 21**. *Microstaurus chiastus* (Worsley) Grün; XP, Sample 149-901A-3R-1, 2 cm; FSU-FO41-D23 and Ph, FSU-FO41-D24. **22, 23**. *Grantarhabdus bukryi* Black; XP, Sample 149-901A-5R-1, 31 cm; FSU-FO46-D34 and Ph, FSU-FO46-D35. **24, 25**. *Cretarhabdus conicus* Bramlette and Martini; XP, Sample 149-901A-3R-1, 33 cm; FSU-FO47-D44 and Ph, FSU-FO47-D2. **26, 27**. *Miravetesina favula* Grün; XP, Sample 149-901A-5R-1, 31 cm; FSU-FO46-D8 and Ph, FSU-FO46-D9.

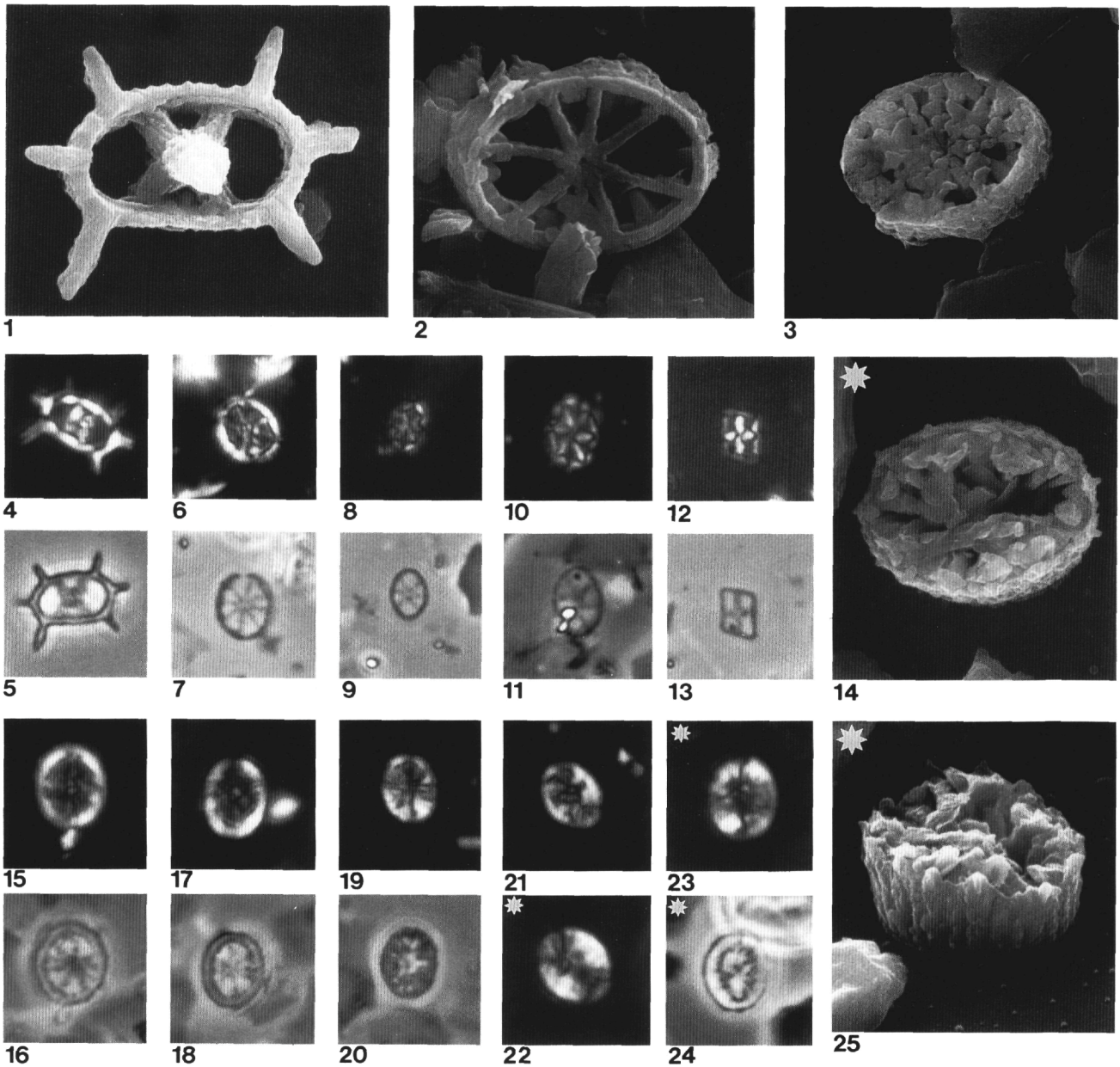


Plate 9. **1, 4, 5<sup>TR</sup>**. *Stephanolithion bigotii* Deflandre, same specimen, Sample 149-901A-5R-1, 31 cm. (1) Distal view, FSU-F110,  $\times 8000$ . (4, 5) XP, FSU-FO52-D20 and Ph, FSU-FO52-D21. **2, 6, 7**. *Stradnerlithus asymmetricus* (Rood, Hay and Barnard) Noël. (2) Proximal view, Sample 149-901A-5R-1, 31 cm, FSU-F47,  $\times 10000$ . (6, 7) XP, Sample 149-901A-5R-1, 74 cm; FSU-FO39-D24 and Ph, FSU-FO39-D25. **8, 9**. *Stradnerlithus sexiramatus* (Pienaar) Perch-Nielsen; XP, Sample 149-901A-5R-1, 31 cm; FSU-FO49-D2 and Ph, Sample 149-901A-5R-1, 74 cm; FSU-FO46-D24. **10, 11**. *Truncatoscapus senarius* (Wind and Wise) Perch-Nielsen 1984, XP, Sample 149-901A-5R-1, 74 cm; FSU-FO49-D4 and Ph, FSU-FO49-D5. **12, 13**. *Diadorhombus scutulatus* (Medd) Medd, XP, Sample 149-901A-7R-1, 14 cm; FSU-FO51-D42 and Ph, FSU-FO51-D43. **3, 15-18**. *Rotelapillus radians* Noël. (3) Proximal view, Sample 149-901A-5R-1, 31 cm, FSU-F5,  $\times 8000$ . (15, 16) XP, Sample 149-901A-5R-1, 74 cm; FSU-FO49-D8 and Ph, FSU-FO49-D9. (17, 18) XP, Sample 149-901A-5R-1, 31 cm; FSU-FO46-D28 and Ph, FSU-FO46-D29. **14, 19-25**. *Rotelapillus pleoseptatus* sp. nov.; Sample 149-901A-5R-1, 31 cm. (14, 22-25)<sup>TR</sup>. Holotype, same specimen. (14) Distal view, FSU-F52,  $\times 8000$ . (25) Oblique distal view, FSU-F56,  $\times 8000$ . (22-24) XP (at 45°) FSU-FO51-D8, XP (at 90°) FSU-FO51-D9, and Ph, FSU-FO51-D10. (19-21) XP (at 90°), FSU-FO45-D9, Ph, FSU-FO45-D11, and XP (at 45°), FSU-FO45-D10.

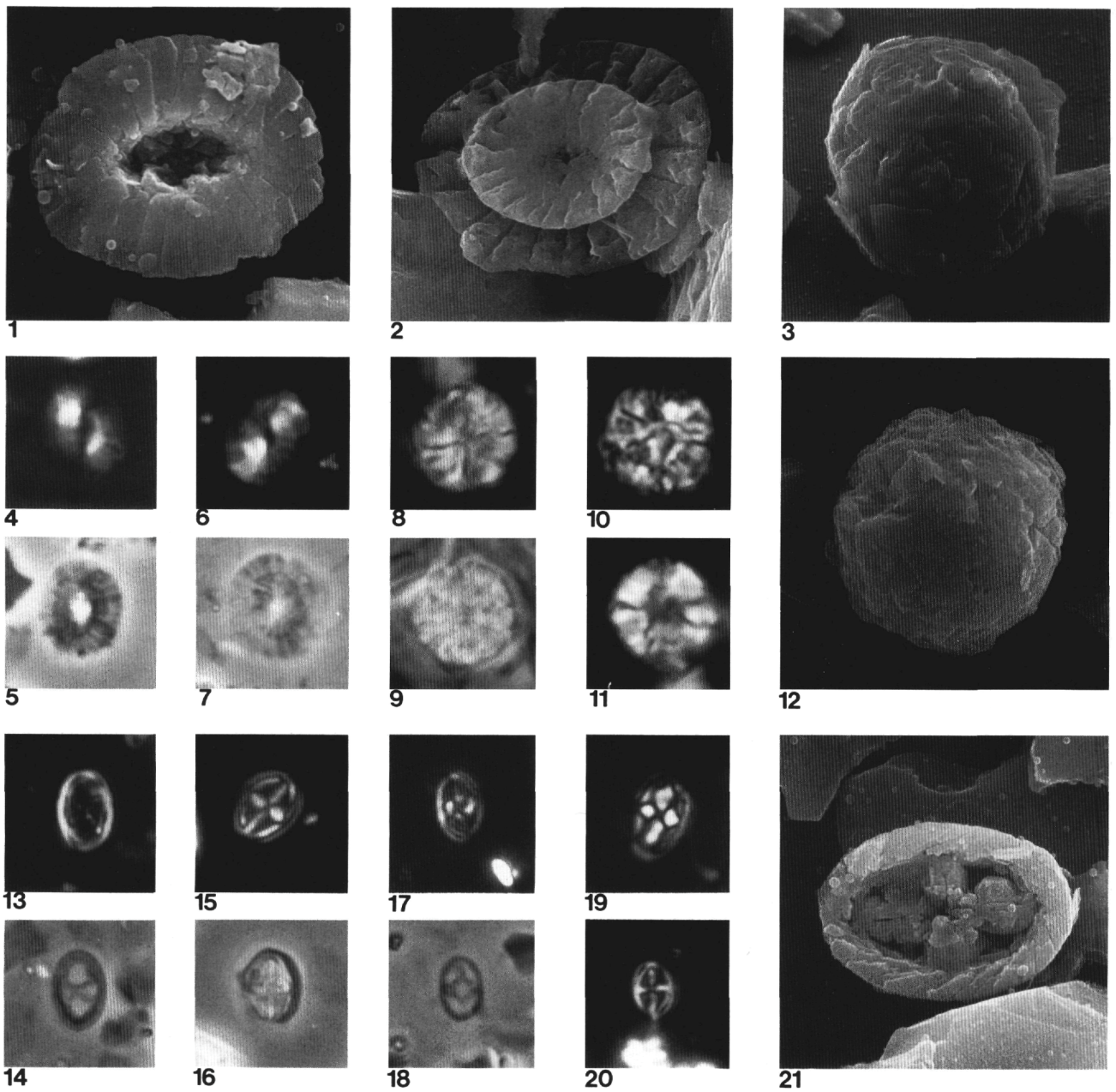


Plate 10. **1, 2, 4-7.** *Markalius ellipticus* Grün. (1, 4, 5)<sup>TR</sup> Same specimen, Sample 149-901A-5R-1, 31 cm.l. Distal view, FSU-F80, ×8000. (4, 5) XP, FSU-FO51-D5 and Ph, FSU-FO51-D6. (2) Proximal view, Sample 149-901A-5R-1, 31 cm; FSU-F9, ×8000. (6, 7) XP, Sample 149-901A-5R-1, 31 cm; FSU-FO44-D35 and Ph, FSU-FO44-D36. **3, 8-12.** *Thoracosphaera* sp. 1. (3, 10, 12)<sup>TR</sup>. Same specimen, Sample 149-901A-5R-1, 31 cm. (3) Side view, FSU-F72, ×6000. (12) Top view, FSU-F73, ×6000. (10) XP, FSU-FO51-D28. (8, 9) XP, Sample 149-901A-5R-1, 31 cm; FSU-FO46-D19 and Ph, FSU-FO46-D20. (11) XP, Sample 149-901A-3R-1, 33 cm; FSU-FO47-D28. **13, 14.** *Chiastozygus leptostaurus* Cooper; XP, Sample 149-901A-5R-1, 31 cm; FSU-FO45-D1, and Ph, FSU-FO45-D2. **15, 16.** *Vagalapilla* sp. 1; XP, Sample 149-901A-5R-1, 31 cm; FSU-FO44-D11, and Ph, FSU-FO44-D12. **17, 18.** *Vagalapilla quadriarculla* (Noël) Roth; XP, Sample 149-901A-5R-1, 74 cm; FSU-FO49-D14, and Ph, FSU-FO49-D15. **19, 21**<sup>TR</sup>. *Vagalapilla* sp. 3; same specimen, Sample 149-901A-5R-1, 31 cm. (21) Distal view, FSU-F75, ×8000. (19) XP, FSU-FO51-D27. **20.** *Vagalapilla stradneri* (Rood, Hay, and Barnard) Thierstein; XP, Sample 149-901A-5R-1, 31 cm; FSU-FO44-D29.

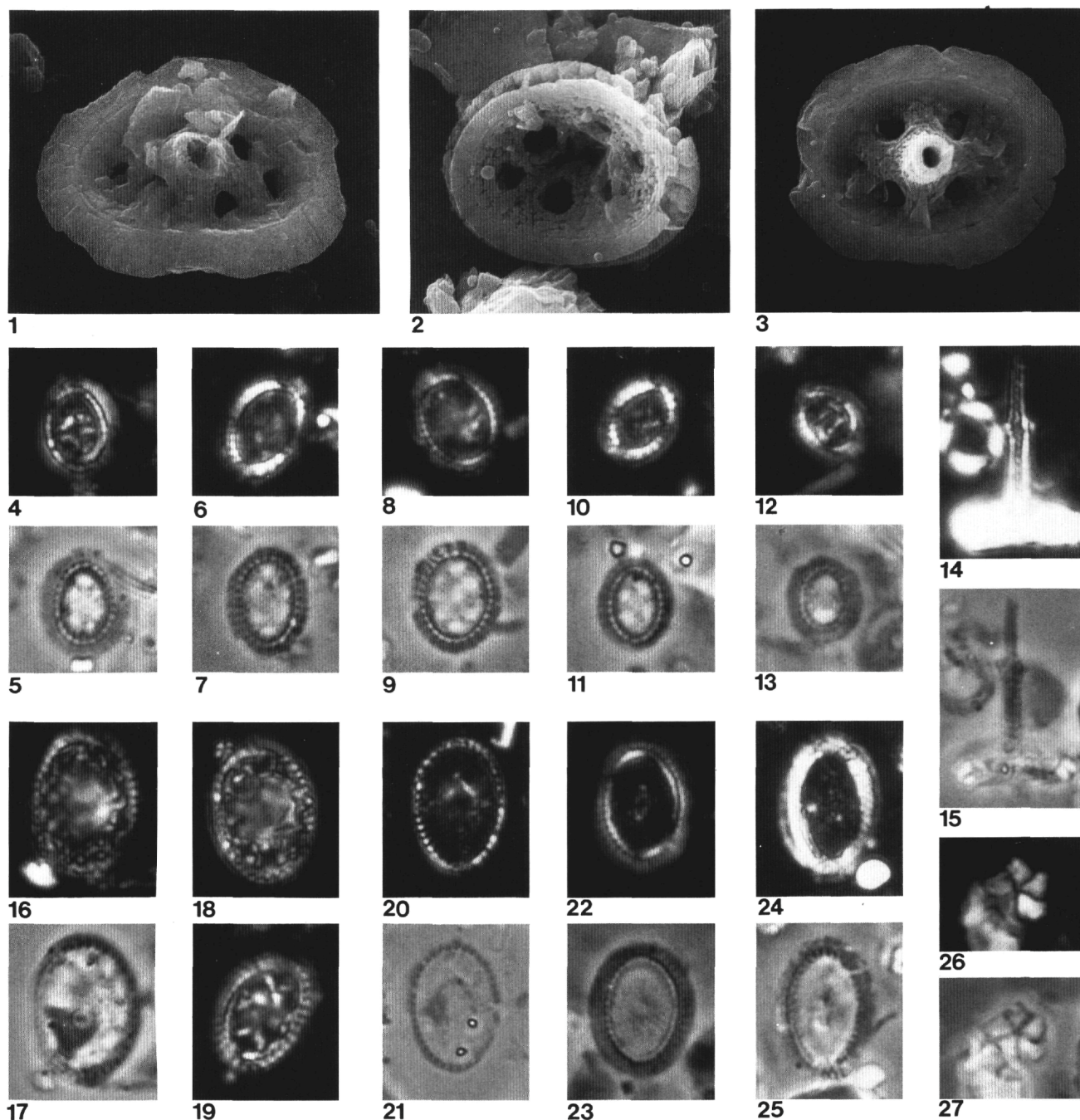


Plate 11. **1, 2, 4-7.** *Hexapodorhabdus cuvillieri* Noël. (1) Distal view, Sample 149-901A-5R-1, 31 cm, FSU-F28,  $\times 6000$ . (2) Proximal view, Sample 149-901A-5R-1, 31 cm, FSU-F50,  $\times 6000$ . (4, 5) Distal view extinction pattern, XP, Sample 149-901A-3R-1, 33 cm; FSU-FO47-D17, and Ph, FSU-FO47-D18. (6, 7) Proximal view extinction pattern, XP, Sample 149-901A-3R-1, 2 cm; FSU-FO41-D13, and Ph, FSU-FO41-D14. **8, 9.** *Octopodorhabdus praevisus* Noël; Sample 149-901A-5R-1, 31 cm; XP, FSU-FO39-D18, and Ph, FSU-FO39-D19. **3, 10, 11.** *Axopodorhabdus cylindratus* (Noël) Wind and Wise. (3) Distal view, Sample 149-901A-5R-1, 31 cm; FSU-F99,  $\times 6000$ . (10, 11) XP, Sample 149-901A-3R-1, 2 cm; FSU-FO41-D8, and Ph, FSU-FO41-D9. **12, 13.** *Tetrapodorhabdus coptensis* Black; XP, Sample 149-901A-5R-1, 31 cm; FSU-F046-D11, and Ph, FSU-FO46-D12. **14, 15.** *Axopodorhabdus rahla* (Noël) Grün and Zweili; XP, Sample 149-901A-5R-1, 31 cm; FSU-FO44-D8, and Ph, FSU-FO44-D10. **16-18.** *Duplexipodorhabdus plethotretus* (Wind and Cepek) Varol and Girgis. (16, 17) XP, Sample 149-901A-5R-1, 31 cm; FSU-FO44-D22, and Ph, FSU-FO44-D23. (18) XP, Sample 149-901A-3R-1, 33 cm; FSU-FO47-D4. **19.** *Perissocyclus noeliae* Black; XP, Sample 149-901A-5R-1, 31 cm; FSU-FO46-DO. **20, 21.** *Ethmorhabdus rimosus* Grün and Zweili; XP, Sample 149-901A-5R-1, 31 cm; FSU-FO45-D20, and Ph, FSU-FO45-D21. **22, 23.** *Ethmorhabdus gallicus* Noël; XP, Sample 149-901A-5R-1, 74 cm; FSU-FO49-D37, and Ph, FSU-FO49-D38. **24, 25.** *Ethmorhabdus hauteriviana* (Black) Applegate, Covington, and Wise; XP, Sample 149-901A-3R-1, 33 cm; FSU-FO47-D23, and Ph, FSU-FO47-D24. **26, 27.** *Braarudosphaera regularis* Black; XP, Sample 149-901A-5R-1, 31 cm; FSU-FO45-D22, and Ph, FSU-FO45-D23.